Euscorpius

Occasional Publications in Scorpiology

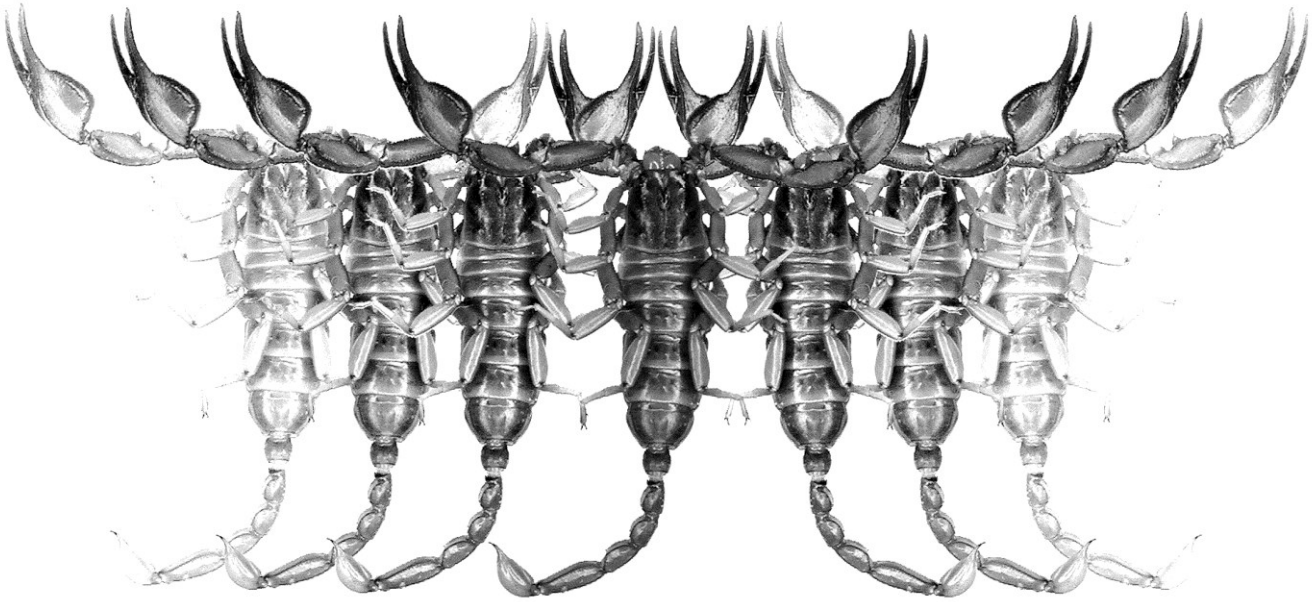

New Analysis of the Genus *Pseudouroctonus* with the Description of Two New Species (Scorpiones: Vaejovidae)

Richard F. Ayrey and Michael E. Soleglad

December 2015 — No. 211

Euscorpius

Occasional Publications in Scorpiology

EDITOR: Victor Fet, Marshall University, 'fet@marshall.edu'
ASSOCIATE EDITOR: Michael E. Soleglad, 'soleglad@znet.com'

Euscorpius is the first research publication completely devoted to scorpions (Arachnida: Scorpiones). ***Euscorpius*** takes advantage of the rapidly evolving medium of quick online publication, at the same time maintaining high research standards for the burgeoning field of scorpion science (scorpiology). ***Euscorpius*** is an expedient and viable medium for the publication of serious papers in scorpiology, including (but not limited to): systematics, evolution, ecology, biogeography, and general biology of scorpions. Review papers, descriptions of new taxa, faunistic surveys, lists of museum collections, and book reviews are welcome.

Derivatio Nominis

The name ***Euscorpius*** Thorell, 1876 refers to the most common genus of scorpions in the Mediterranean region and southern Europe (family Euscorpiidae).

Euscorpius is located at: **http://www.science.marshall.edu/fet/Euscorpius**
(Marshall University, Huntington, West Virginia 25755-2510, USA)

ICZN COMPLIANCE OF ELECTRONIC PUBLICATIONS:

Electronic ("e-only") publications are fully compliant with ICZN (*International Code of Zoological Nomenclature*) (i.e. for the purposes of new names and new nomenclatural acts) when properly archived and registered. All ***Euscorpius*** issues starting from No. 156 (2013) are archived in two electronic archives:

- **Biotaxa,** http://biotaxa.org/Euscorpius (ICZN-approved and ZooBank-enabled)
- **Marshall Digital Scholar**, http://mds.marshall.edu/euscorpius/. (This website also archives all *Euscorpius* issues previously published on CD-ROMs.)

Between 2000 and 2013, ICZN ***did not accept online texts*** as "published work" (Article 9.8). At this time, *Euscorpius* was produced in two ***identical*** versions: online (*ISSN 1536-9307*) and CD-ROM (*ISSN 1536-9293*) (laser disk) in archive-quality, read-only format. Both versions had the identical date of publication, as well as identical page and figure numbers. ***Only copies distributed on a CD-ROM*** from ***Euscorpius*** in 2001-2012 represent published work in compliance with the ICZN, i.e. for the purposes of new names and new nomenclatural acts.

In September 2012, ICZN Article 8. *What constitutes published work*, has been amended and allowed for electronic publications, disallowing publication on optical discs. From January 2013, ***Euscorpius*** discontinued CD-ROM production; only online electronic version (*ISSN 1536-9307*) is published. For further details on the new ICZN amendment, see http://www.pensoft.net/journals/zookeys/article/3944/.

Publication date: 7 December 2015
http://zoobank.org/urn:lsid:zoobank.org:pub:45EF160B-AA06-4205-ADA3-73DE51A805EF

Euscorpius — Occasional Publications in Scorpiology. 2015, No. 211

New analysis of the genus *Pseudouroctonus* with the description of two new species (Scorpiones: Vaejovidae)

Richard F. Ayrey [1] & Michael E. Soleglad [2]

[1] P. O. Box 2236, Flagstaff, Arizona 86003, USA; email: flagrich@azscorpion.com

[2] 32255 Safflower St., Winchester, California 92596, USA; email: soleglad@znet.com

http://zoobank.org/urn:lsid:zoobank.org:pub:45EF160B-AA06-4205-ADA3-73DE51A805EF

Summary

Two new species of *Pseudouroctonus* are described from southeastern Arizona, USA, *Pseudouroctonus santarita*, **sp. nov.** from the Santa Rita Mountains and *P. kremani*, **sp. nov.** from the Santa Catalina Mountains. These new species are closely related to *P. apacheanus* (Gertsch et Soleglad, 1972). A combination of morphological differences in the hemispermatophore, the mating plug, and several morphometric-based characters are identified as diagnostic. New substructures are identified for the mating plug.

Introduction

Gertsch & Soleglad (1972: 575–577) described *Pseudouroctonus apacheanus* from southeastern Arizona. This species was placed in the genus *Uroctonus* along with *U. mordax* (now in family Chactidae) and twelve other new species also described at the time. Also in the same work, seven new species and subspecies were described and placed in the genus *Vaejovis*, some considered related to *Uroctonus*. The authors listed no less than 21 separate localities for *P. apacheanus*, spanning the states of Arizona, New Mexico, and Texas. Its type locality was listed as 5 miles SW of Portal, Cochise Co., Arizona, in the Chiricahua Mountains.

Bryson et al. (2013: figs. 1–4) presented a molecular-based study of several species and subspecies currently placed in the genus *Pseudouroctonus* which they referred to as the "minimus" complex. Their study divided several populations spanning eight taxa (as represented by genetic samples) into the Northwest (NW) and Southeast (SE) clades. Within the SE clade genetic samples from no less than eleven localities were tentatively identified as *P. apacheanus*, and formed three separate clades, two of which form one larger clade. As in the original Gertsch & Soleglad (1972) paper, these samples were from Arizona, New Mexico, and Texas and included many localities originally reported by Gertsch & Soleglad (1972). The samples from the eleven localities of Bryson et al. (2013: figs. 3–4) formed three separate genetic clades as follows: clade-1, which we refer to here as the "Santa Rita clade", is based on samples from the Santa Rita, Atascosa, and Quinlan mountains; clade-2, the "Chiricahua clade", is composed of samples from the Chiricahua (*P. apacheanus* type locality), Catalina, Pinaleño, and Peloncillo mountains, and clade-3, the "Chiso clade", is based on four samples, all from the southwest corner of Texas (i.e., Guadalupe, Chisos, Davis, and Independence localities). Bryson et al. (2013: fig. 3) estimated that clade-1 separated from the other two clades over 20 Mya, and clade-3 separated from clade-2 approximately 14.51 Mya (mean estimates).

Based on the Bryson et al. (2013) results discussed above, specimens from two of their "*apacheanus*" populations were collected along with topotype specimens of *P. apacheanus* from the Chiricahua mountains: Madera Canyon in the Santa Rita mountains (i.e., clade-1) and Molina Basin in the Catalina mountains (i.e., clade-2). Incidently, Bryson et al. (2013) estimated that the separation of samples from the Chiricahua (type locality) and Catalina mountains was only 8.11 Mya (mean estimate), both are included in clade-2. Specimens from other populations sampled by Bryson et al. (2013) in the three clades discussed above were not examined, so future investigations must be conducted to determine if they also represent new species.

Based on detailed analysis and comparison of the three populations discussed above, we define two new species, *Pseudouroctonus santarita* from the Santa Rita mountains (clade-1) and *P. kremani* from the Catalina mountains (clade-2). New morphological information is illustrated and described for the hemispermatophore mating plug, trichobothrial patterns pertaining in general to *Pseudouroctonus*, and the chelal carinal configuration

unique to most species in this genus. Appendix A provides several trichobothrial patterns from *Pseudouroctonus* and *Uroctonites* species, most published for the first time; and Appendix B provides the complete statistical data for the morphology-based analysis conducted in this paper.

Materials and Methods

Terminology and conventions

Measurements are as described in Stahnke (1971), trichobothrial patterns are as in Vachon (1974), pedipalp finger dentition and chelal carinae follows Soleglad & Sissom (2001), sternum terminology as described in Soleglad & Fet (2003a), cheliceral dentition terminology as described by Soleglad & Fet (2003b), and the hemispermatophore follows Soleglad & Fet (2008).

Abbreviations

RFA, personal collection of Richard F. Ayrey, Flagstaff, Arizona, USA; USNM, United States National Museum, Smithsonian Institution, Washington, DC, USA; ABDSP, Anza-Borrego Desert State Park, San Diego and Riverside Counties, California, USA.

Map generation software package

Map was generated by Earth Explorer 6.1, with positional and altitude data compiled through Google Maps.

Material Examined

In addition to the type material listed for the two new species described in this paper, the following material was also examined.

***Pseudouroctonus apacheanus* (6 specimens)**

Chiricahua Mountains, Rucker Canyon, Arizona, USA, 5 September 2008, leg. R. F. Ayrey, 1 ♂ (RA836, RFA); Chiricahua Mountains, Cave Creek, Arizona, USA, 8 February 2008, leg R. F. Ayrey, 1 ♀ (RA1106, RFA); 16 August 2115, leg. R. F. Ayrey, 1 ♂ (RA2133, RFA); 24 August 2014, leg. R. F. Ayrey, 1 ♀ (RA1107, RFA); 20 August 2012, leg. R. F. Ayrey, 1 ♂ (RA1097, RFA); Chiricahua Mountains, Sunset Campground, Arizona, USA, 2 August 2008, leg R. F. Ayrey, 1 ♀ RA552, RFA).

Structure Analysis

We discuss structures that are important to the taxonomy of the genus *Pseudouroctonus*. In particular, trichobothrial patterns, the pedipalp chela carinal configuration, and the hemispermatophore and its mating plug are considered.

Trichobothrial Patterns

The trichobothrial patterns of *Pseudouroctonus* are quite consistent across a wide number of species currently defined for the genus. See pattern of *P. apacheanus* in Figure 1 for an example. In fact, most of the species included by Bryson et al. (2013) in their molecular-based study of the "*minimus*" complex have trichobothrial patterns consistent with that shown in Figure 1 (see Appendix A). When we say consistent, we are referring to even subtle positions of most or *all* of the trichobothria, and some of these specific locations are diagnostic. This is significant for several reasons. First, it is another testimony to the importance of trichobothria in the overall systematics of scorpions --- predictable consistency. Second, we also see species currently placed in genus *Pseudouroctonus* that are not consistent in all trichobothrial locations.

The trichobothrial pattern of genus *Pseudouroctonus* exhibits several postional-based diagnostic characters: for the chela, trichobothria *ib*-*it* are positioned quite basal on the fixed finger/palm juncture, *ib* is located on the palm and *it* located on the finger base; fixed finger trichobothrium *eb* is adjacent to the fixed finger juncture; chelal V_4 is located on the *V1* carina; *Db* is located dorsal to the *D1* carina; *Dt* is positioned well on the proximal half of the palm; and for the patella, v_3 is located adjacent to et_3. Of the eight species and subspecies included in Bryson's et al. (2013) study, only *P. savvasi*, a troglobitic species found in caves in Coahuila, Mexico, differs in two positions as depicted by its authors: trichobothrium *Db* is positioned on the *D1* carinae, not dorsal of; and patellar trichobothrium v_3 is located proximal to et_3 (see Fig. A-6 in Appendix A). Also compare the three trichobothria patterns illustrated in this paper with the fourteen patterns provided in Appendix A.

In contrast, four trichobothria-based diagnostic characters were presented by Soleglad, Fet & Graham (2014: 3; fig. 1) in their definition of genus *Kovarikia*, characters not found in *Pseudouroctonus*: neobothriotaxy found on the chelal ventral surface; the most basal chelal ventral trichobothrium not located on the V_1 carina, but instead on the ventral surface; the angle formed by Est_1 and V_1 is slanted proximally, not parallel to the articular membrane of the fixed finger; and *Est* and *Dt* situated more mid-palm. Tate et al. (2013: fig. 16), in their definition of *P. peccatum*, show a pattern that also exhibits some differences from that of *P. apacheanus*. Impart, due to its elongated chelal fingers, we see that the *ib*-*it* series is not position as basal as in *Pseudouroctonus*, both trichobothria found on the fixed

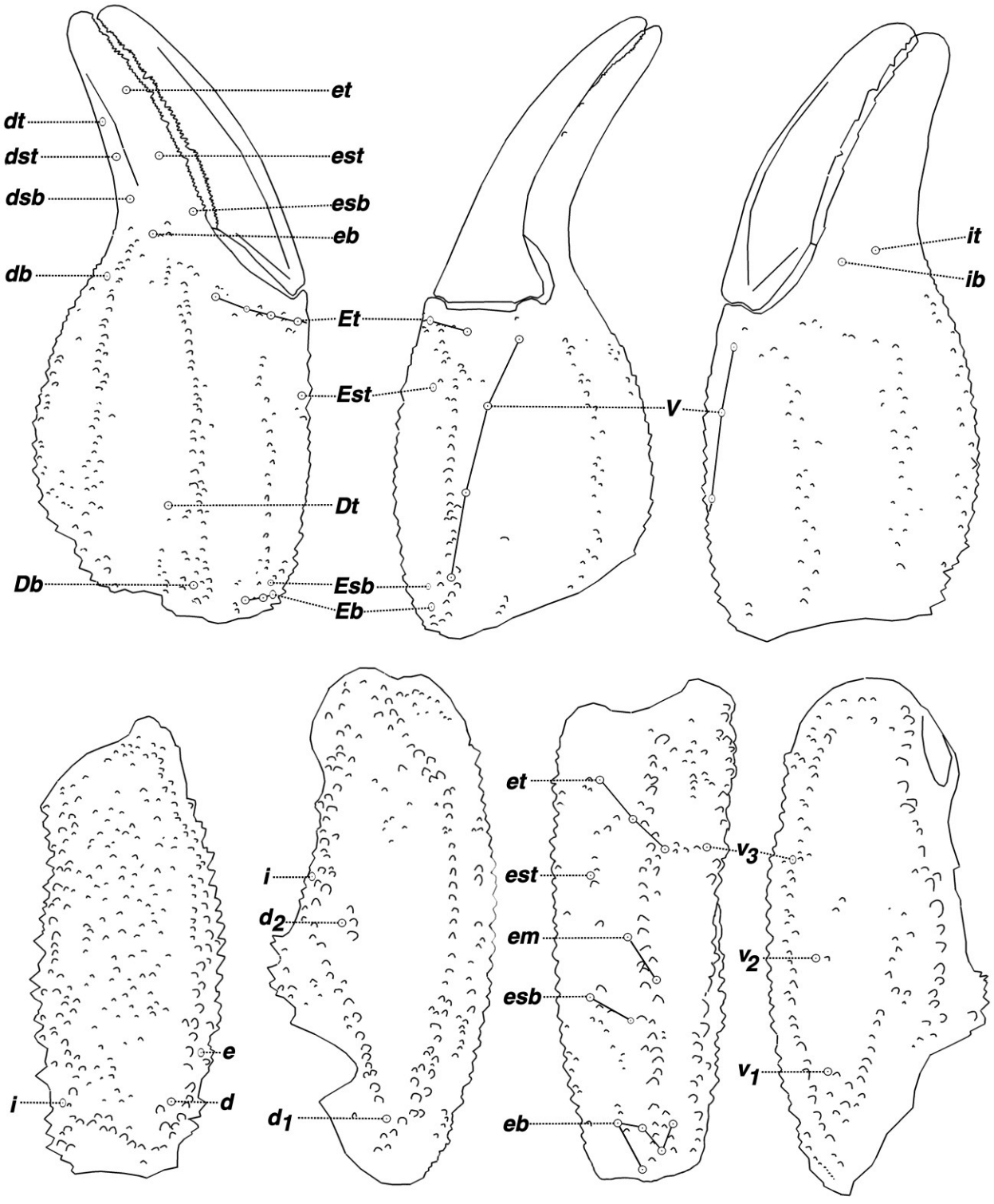

Figure 1: *Pseudouroctonus apacheanus*, male, Rucker Canyon, Chiricahua Mountains, Arizona, USA. Trichobothrial pattern.

finger base. Similarly, the fixed finger trichobothrium *db* is distal of the finger juncture. It is noteworthy to state here, that these differences are also observed in the most easternmost species *P. reddelli* and its close relative, *P. sprousei*, both troglomorphic species. Again, these species have relatively elongated fingers.

In addition to the illustrations of trichobothrial patterns shown in Figure 1 and of the two new species

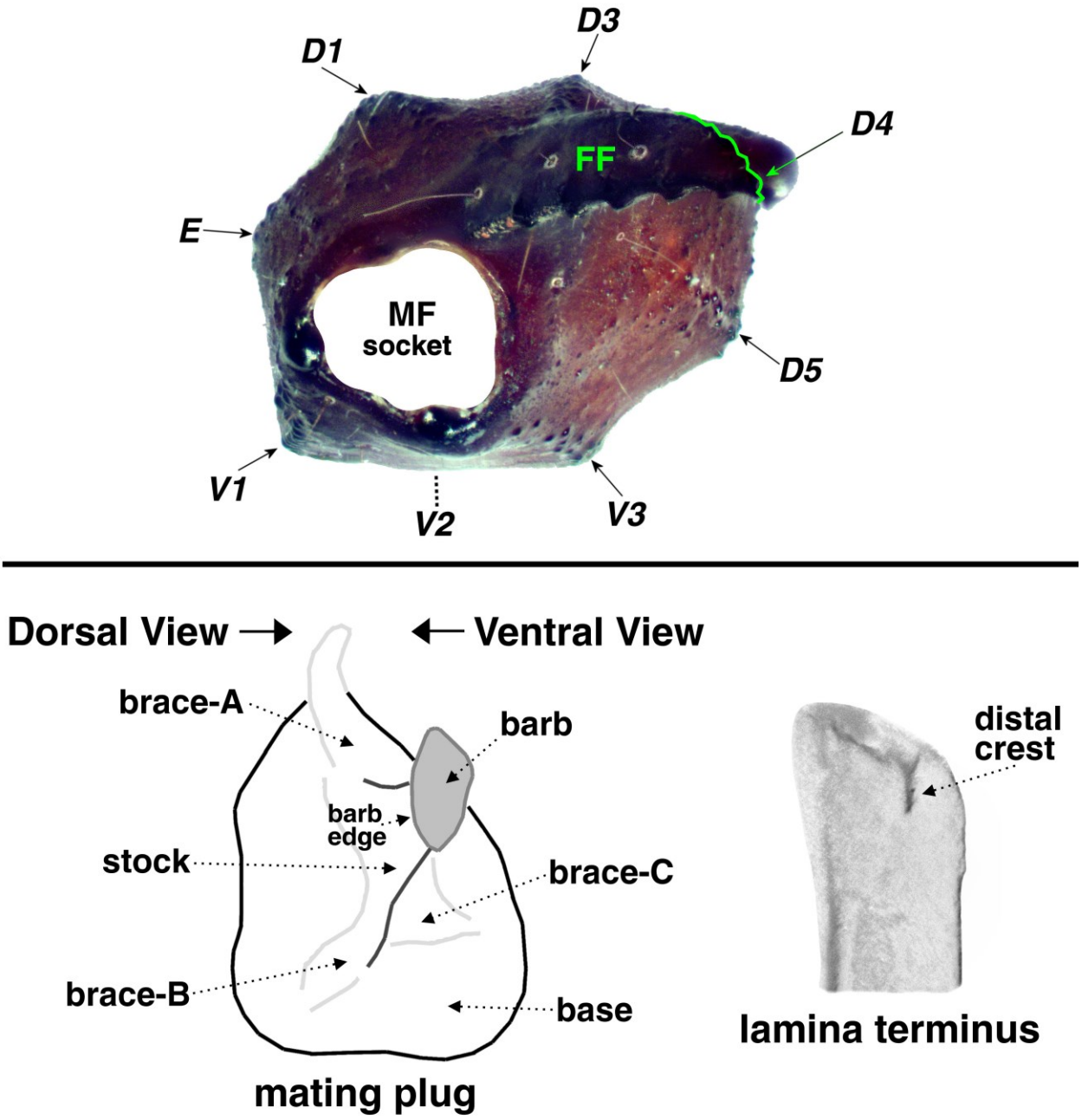

Figure 2: Top. Distal perspective of the right pedipalp chela of *Pseudouroctonus apacheanus*, male, showing the typical carinal configuration found in the genus *Pseudouroctonus*. Of particular importance are the essential absence of the ventromedian carina (*V2*) and the flat orientation of the dorsosecondary (*D3*) carina, combined making the two planes *D1|D3|D4* and *V1|V2|V3* essentially parallel. Note, the green line indicates the *D4* carina which is blocked from view by the fixed finger terminus. MF = movable finger, FF = fixed finger, *D1* = digital carina, *D3* = dorsosecondary carina, *D4* = dorsomarginal carina, *D5* = dorsointernal carina, *V1* = ventroexternal carina, *V2* = ventromedian carina, *V3* = ventrointernal carina, and *E* = exterosecondary carina. Note, the subdigital carina (*D2*), which is vestigial, is not shown. **Bottom.** Diagrammatic view of the hemispermatophore mating plug and lamina terminus of *Pseudouroctonus santarita* **sp. nov.** Annotated diagram identifies substructures of the mating plug (internal view), and the lamina terminus (dorsal view).

described in this paper, we provide fourteen additional patterns in Appendix A, most published for the first time. These trichobothrial patterns include the following: all species and subspecies addressed by Bryson et al. (2013) with the exception of subspecies *P. minimus minimus*; *P. reddelli, P. sprousei*, *P. iviei* and *P. glimmei*; a distant relative *P. lindsayi*; and three species of *Uroctonites*. These patterns should be compared to the

trichobothrial patterns published for the three species comprising genus *Kovarikia* by Soleglad, Fet & Graham (2014: figs. A-1–A-3) and *P. peccatum* by Tate et al. (2013: fig. 16).

Pedipalp Chelal Carinae

In the genus *Pseudouroctonus* the overall shape of the chelal palm is an important diagnostic character at the genus level and higher. The shape is dictated by the alignment and relative development of its carinae. In particular for *Pseudouroctonus*, the somewhat low-profile development of the dorsosecondary (*D3*) carina combined with the absence of the ventromedian (*V2*) carina forces the overall shape of the palm to have a somewhat flat appearance when viewed from the fingers. In Figure 2 we see the chela of *P. apacheanus* from a distal perspective (i.e., from the fingers). It is clear from this Figure that *D3*'s profile is quite low when compared to the other fixed finger carinae, caused mostly by the obtuse angles it forms with the interconnecting areas. Similarly, *V2*'s absence conspicuously forces the plane *V1|V2|V3* to be flat. The overall affect is that the planes *D1|D3|D4* and *V1|V2|V3* are essentially subparallel.

It is important to note (based on preliminary cladistic analysis) that the clade *P. glimmei* + *P. iviei* does not comply to this organization of parallel planes, the chelal shape more typical of other vaejovids, carinae *D3* and *V2* well developed, especially *V2* (see chela carinal diagram of *P. iviei* in Soleglad (1973: fig. 12)). Also, the subdigital carina (*D2*), which is usually vestigial in most vaejovids, is more developed, comprised of six or more granules (also note, Soleglad & Fet, 2008: 103, reported a well developed *D2* carina for genera *Kochius* and *Thorellius*, forming subtribe Thorelliina). These observations are particularly important in conjunction with Soleglad, Fet & Graham's (2014: 5) observation that these two species also have a secondary lamellar hook on the hemispermatophore, only observed in genus *Kovarikia*. It is also important to note, that both *P. glimmei* and *P. iviei* occur the most northern of any of the *Pseudouroctonus* species, occurring in northern California. In fact, these two species, *P. iviei* in particular, occur further north than any species in genus *Vaejovis* (both genera being members of the subfamily Vaejovinae).

Soleglad (1973: figs. 4–12) first illustrated the unique shape of the chelal palm found in genus *Pseudouroctonus* (and in other genera) where it was compared to other vaejovid chelal shapes. Stockwell (1991: 416, figs. 46–47) also used this diagnostic character to identify, in part, genera *Uroctonus*, *Pseudouroctonus*, and *Uroctonites*. Finally, Soleglad & Sissom (2001: fig. 44) used this same character to distinguish the family Euscorpiidae from Chactidae. As with *Pseudouroctonus*, the same chelal carinae, *D3* and *V2*, were involved. It is clear that this is an important diagnostic character since it involves major morphological differences in the pedipalp chela occurring in multiple groups of scorpions.

Hemispermatophore and Mating Plug

The hemispermatophore provides important diagnostic information at several levels of scorpion systematics. The four fundamental hemispermatophore types are found at the highest levels of scorpion taxonomy, the same levels where the four trichobothrial types are defined. At lower levels, such as the vaejovids, and in particular, in the genus *Pseudouroctonus* and its close relatives (e.g., *Kovarikia*) the hemispermatophore and its mating plug provide key diagnostic information both at the genus and species level.

Mating Plug. The hemispermatophore and its mating plug provide important diagnostic information for our analysis of the two new species described below as contrasted with *P. apacheanus*. The mating plug, in particular, has proved to be valuable in this analysis. The adult male of the three species discussed in this paper are somewhat small in size, their lengths ranging 25–30 mm. The mating plug found in these species is very small, roughly 0.35 mm in length (i.e., distance between its base and the barb). The terminology followed in this paper was first established, in part, by Soleglad & Fet (2008: fig. 40). This terminology has been further augmented in this paper based on new analysis of the mating plug.

In Figure 2 we illustrate the mating plug's substructures. The views depicted in this Figure and discussed below are based on the mating plug's position as embedded in the hemispermatophore's median area. In the annotated diagram we show the mating plug from its internal aspect. Therefore the mating plug's barb is the closest to the viewing plane, which when embedded in the hemispermatophore, faces the internal aspect where the lamellar hook is located.

The mating plug is composed of three primary components, the *base*, *stock*, and *barb*, and three secondary components, *brace-A*, *brace-B*, and *brace-C*. The mating plug *base* is a somewhat flat structure shaped like an irregular rounded triangle. Its internal surface is slightly convexed and its external surface slightly concaved. Connected to the base is the *stock*, an irregular shaped substructure that tapers as it extends towards the barb. It is somewhat flatten on both its dorsal and ventral aspects. Three substructures, termed *braces* in this paper, provide support for the *stock* where it connects to the *base*. Each *brace* extends towards one of the three rounded vertices of the *base* as follows: *brace-A* connects to the vertex pointing towards the hemispermato-

Figure 3: *Pseudouroctonus santarita*, **sp. nov**., Madera Canyon, Santa Rita Mtns., Pima Co., Arizona, USA. **Top.** Paratype female in natural habitat. **Bottom.** Paratype male in natural habitat.

phore's lamina, *brace-B* connects to the vertex which points towards the hemispermatophore's trunk, and *brace-C* connects to the vertex which points towards the ventral surface of the hemispermatophore. *Braces-A* and *-B* are connected to the wided edges of the stock and *brace-C* connects to the flattened ventral surface of the *stock*. The *barb* attaches to the terminus of the *stock*. From an internal perspective, the *barb* is formed as an irregular elongated curved ellipse. The elongated portions of the *barb* are aligned with the widened edges of the *stock*, the portion that points towards the hemispermatophore lamina is slightly longer than the portion pointing towards the trunk. The *barb*'s edge, which is smooth and points to the dorsal surface, extends from the *stock* and curves somewhat towards the *base*.

Finally, depending on the species, the *stock* and *braces* exhibit additional projections which are diagnostic. These will be discussed below in the new species descriptions and comparisons.

Distal Crest. Occurring in several vaejovid species (see list below) is a small substructure on the hemispermatophore lamina terminus which we term as a *distal crest*. In Figure 2 we illustrate this crest. It is a small sclerotized ridge occurring on the internal aspect of the dorsal surface of the lamina terminus.

The distal crest has been reported in the vaejovids for the following species, all members of subfamily Vaejovinae: *Vaejovis rossmani* (Sissom, 1989: fig. 76), *V. monticola* (Sissom, 1989: fig. 78), *V. sprousei* (Gonzalez et al., 2004: fig. 1), *V. norteno* (Sissom & Gonzalez, 2004: fig. 1), *V. chisos* (Jarvis et al., 2004: fig. 1), *V. lapidicola* (Soleglad & Fet, 2008: fig. 71), *V. crumpi* (Ayrey & Soleglad, 2011: fig. 18), *V. halli* (Ayrey, 2012: fig. 11), *V. trinityae* (Ayrey, 2013: fig. 11), *Pseudouroctonus peccatum* (Tate et al., 2013: fig. 17), *V. grahami* (Ayrey & Soleglad, 2014: fig. 12), *V. grayae* (Ayrey, 2014: fig. 10), *V. coalcoman* (Contreras & Francke , 2014: p. 27), and *Vaejovis tenamaztlei* (Contreras, Francke & Bryson, 2015: fig. 12–13). In this paper we report and illustrate the distal crest for *Pseudouroctonus apacheanus* and *P. santarita*, **sp. nov**.

We must stress here that the distal crest discussed for the vaejovids is not necessarily homologous to the more substantial crest occurring in many bothriurid species, although they do both occur on the dorsal surface of the lamina terminus. For examples see the left hemispermatophore illustrated for species *Urophonius mondacai* in Kovařík & Ojanguren Affilastro (2013: fig. ZJ-2), *Orobothriurus grismadoi* in Ojanguren Affilastro et al. (2009: fig. 17), *Bothriurus sanctaecrucis* in Mattoni (2007: fig. 25), and *Brachistosternus coquimbo* in Ojanguren Affilastro et al. (2007: fig. 12).

Systematics

Order **SCORPIONES** C. L. Koch, 1850
Suborder Neoscorpiones Thorell et Lindström, 1885
Infraorder Orthosterni Pocock, 1911
Parvorder Iurida Soleglad et Fet, 2003
Superfamily Chactoidea Pocock, 1893
Family Vaejovidae Thorell, 1876
Subfamily Vaejovinae Thorell, 1876
Genus *Pseudouroctonus* Stahnke, 1974

***Pseudouroctonus santarita* Ayrey et Soleglad, sp. nov.**
(Figs. 3–16; Table 1)
http://zoobank.org/urn:lsid:zoobank.org:act:A73E4F1A-C44D-464D-899E-50DA6DD03E28

REFERENCES:
Uroctonus apacheanus: Gertsch & Soleglad, 1972: 576, 577 (in part).
Pseudouroctonus apacheanus: McWest, 2009: fig. 12; Bryson et al., 2013: 5, 6, figs. 1, 2.

Type material: Holotype ♀, Madera Canyon, Santa Rita Mountains, Santa Cruz County, Arizona, USA (31.71325, -110.87507; 1641 m asl.), 5 September 2008, leg. R. F. Ayrey, (#353, USNM); paratype ♂, same locality, 13 July 2014, leg. R.F. Ayrey, (#953, USNM); Paratypes ♀, 2 miles west of Pena Blanca Lake, Atascosa Mountains, Santa Cruz County, Arizona, USA, 1 March 2009, leg. T. Miscione, (#551, RFA); ♀, east side of the Santa Rita Mountains, southwest of Patagonia, Santa Cruz County, Arizona, USA, 12 April 2014, leg. T. Miscione, (#1160, RFA); ♀, Ruby Road, Pajarito Mountains, Santa Cruz County, Arizona, USA, 1 March 2009, leg. T. Miscione, (#213, RFA); ♀, off Harshaw Road, Patagonia Mountains, Santa Cruz County, Arizona, USA, 25 July 2008, leg. R. Troup, (#1100, RFA).

Diagnosis. Small species with heavy chelae, 24–29 mm. Pectinal tooth counts 10–12 males, 8–10 females; metasoma stocky, segments III–V length to width ratio 0.95–1.00, 1.22–1.32, and 2.16–2.22 in males, 0.90–0.95, 1.18–1.23, and 2.05–2.12 in females; metasomal segments IV–V widths to fixed finger length ratio 0.86–0.93 and 0.84–0.85 in males, 0.83–0.86 and 0.79–0.83 in females; fixed finger *MD* counts 46–50 for males and 47–53 for females; hemispermatophore lamina terminus with distal crest; mating plug brace-A and brace-B with projections.

Distribution. Santa Rita Mountains, southern Arizona, USA. See map in Fig. 33.

Etymology. Named after the Santa Rita Mountains in southern Arizona, USA, from where the species was originally collected.

FEMALE. The following description is based on holotype female from the Santa Rita Mountains, Arizona, USA. Measurements of the holotype female and paratype male are presented in Table 1. See Figure 3 for photographs of live paratype female and male specimens.

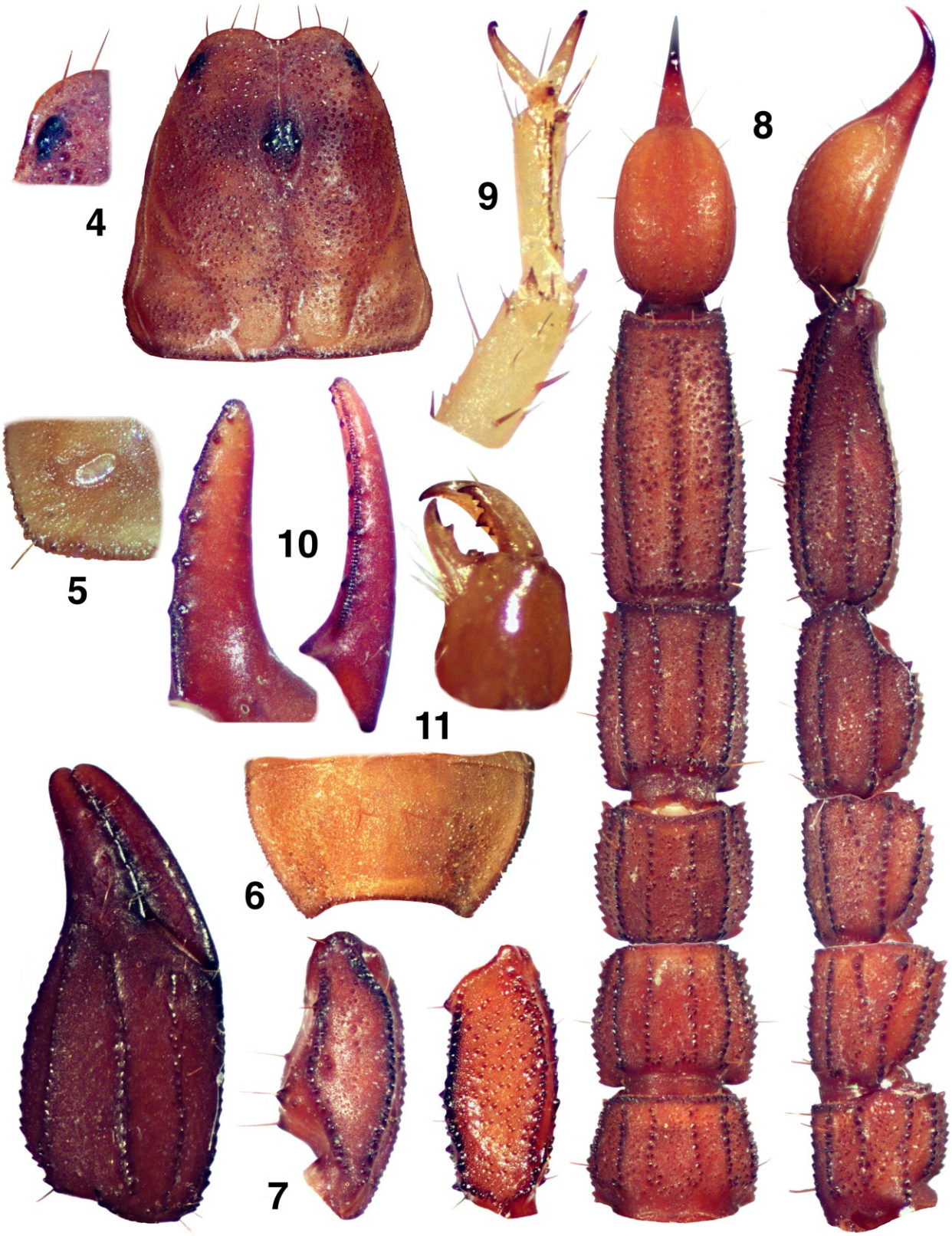

Figures 4–11: *Pseudouroctonus santarita*, **sp. nov**. **Figs. 4–8.** Holotype female. **Figs. 9–11.** Paratype male. **4.** Carapace and closeup of left lateral eyes. **5.** Right stigma III. **6.** Sternite VII. **7.** Right chela, patella and femur. **8.** Metasoma and telson, ventral and lateral views. **9.** Right leg III, ventral view. **10.** Fixed and movable finger dentition. **11.** Chelicera, dorsal view, showing smooth ventral edge.

Figure 12: *Pseudouroctonus santarita*, **sp. nov**. Sternopectinal area of holotype female (left) and paratype male (right).

COLORATION. The posterior half of the carapace and mesosoma orange-brown; carapace anterior half a darker brown. Metasoma dark brown with darker carinae; telson vesicle orange. Pedipalps dark brown with darker carinae. Sternopectinal area and sternites light brown; legs brown.

CARAPACE (Fig. 4). Anterior edge with a conspicuous narrow median indentation, providing a ratio of 0.033 when its depth is compared to the carapace's length; edge with six setae visible; entire surface densely covered with medium sized granules. Three lateral eyes are present, the posterior eye considerably smaller. Median eyes and tubercle of medium size, positioned anterior of middle with the following length and width ratios: 0.351 (anterior edge to medium tubercle middle / carapace length) and 0.164 (width of median tubercle including eyes / width of carapace at that point).

MESOSOMA (Figs. 5–6). Tergites I–VII densely covered with small granules; tergite VII lateral and median carinae strong and crenulate. Sternites III–V smooth, VI–VII with small dense granules on posterior lateral aspects; sternite VII with weak irregularly granulated lateral carinae and obsolete median carinae (Fig. 6). Stigmata (Fig. 5) are small to medium in size and elliptical in shape.

METASOMA (Fig. 8). Segment I–III wider than long. Segments I–IV: dorsal and dorsolateral carinae serrated; dorsal and dorsolateral (I–III) carinae terminate with an enlarged spine; lateral carinae serrated on I, serrated on posterior two-thirds of II and posterior one-half on III, oboslete on segment IV; ventrolateral and ventromedian carinae serrated. Dorsolateral carinae of segment IV terminate essentially at the articulation condyle. Segment V: dorsolateral carinae rounded and granulated; lateral carinae serrated for two-thirds of posterior aspect; ventrolateral and single ventromedian carinae serrated; ventromedian carina not bifurcated, terminating in straight line. Anal arch with 14 small granules. Intercarinal areas of segments I–V scattered with minute granules.

TELSON (Fig. 8). Vesicle fairly robust with some low-profile granules located on the ventral surface; moderate setation on ventral surface. Aculeus with medium curve, well delineated from the vesicle when viewed ventrally. Vesicular tabs with a single small curved spine.

PECTINES (Fig. 12, paratype male). Well-developed segments exhibiting length / width ratio 2.474 (length taken at anterior lamellae / width at widest point including teeth). Sclerite construction complex, three anterior lamellae and six middle lamella; fulcra of medium development. Teeth number 10/10. Sensory areas developed along most of tooth inner length on all teeth, including basal tooth. Scattered setae found on anterior lamellae and distal pectinal tooth. Basal piece large, with well developed wide indentation along anterior edge, length / width ratio 0.575.

GENITAL OPERCULUM (Fig. 12). Sclerites triangular, wider than long, separated on posterior one-third.

STERNUM (Fig. 12). Type 2, posterior emargination present, well-defined convex lateral lobes, apex shallow; sclerite wider than long, in ratio 0.833.

CHELICERAE (Fig. 11). Movable finger dorsal edge with two subdistal (*sd*) denticles; ventral edge smooth with well developed serrula on distal half (with 25–30 tines). Ventral distal denticle (*vd*) slightly longer than dorsal (*dd*). Fixed finger with four denticles, median (*m*) and basal (*b*) denticles conjoined on common trunk; no ventral accessory denticles present.

PEDIPALPS (Figs. 7, 10, 13). Well-developed chelae, with short fingers, carinae well developed, no scalloping on the fingers. Planes formed by carinae *D1|D3|D4* and *V1|V2|V3* are essentially parallel. **Femur:** Dorsointernal

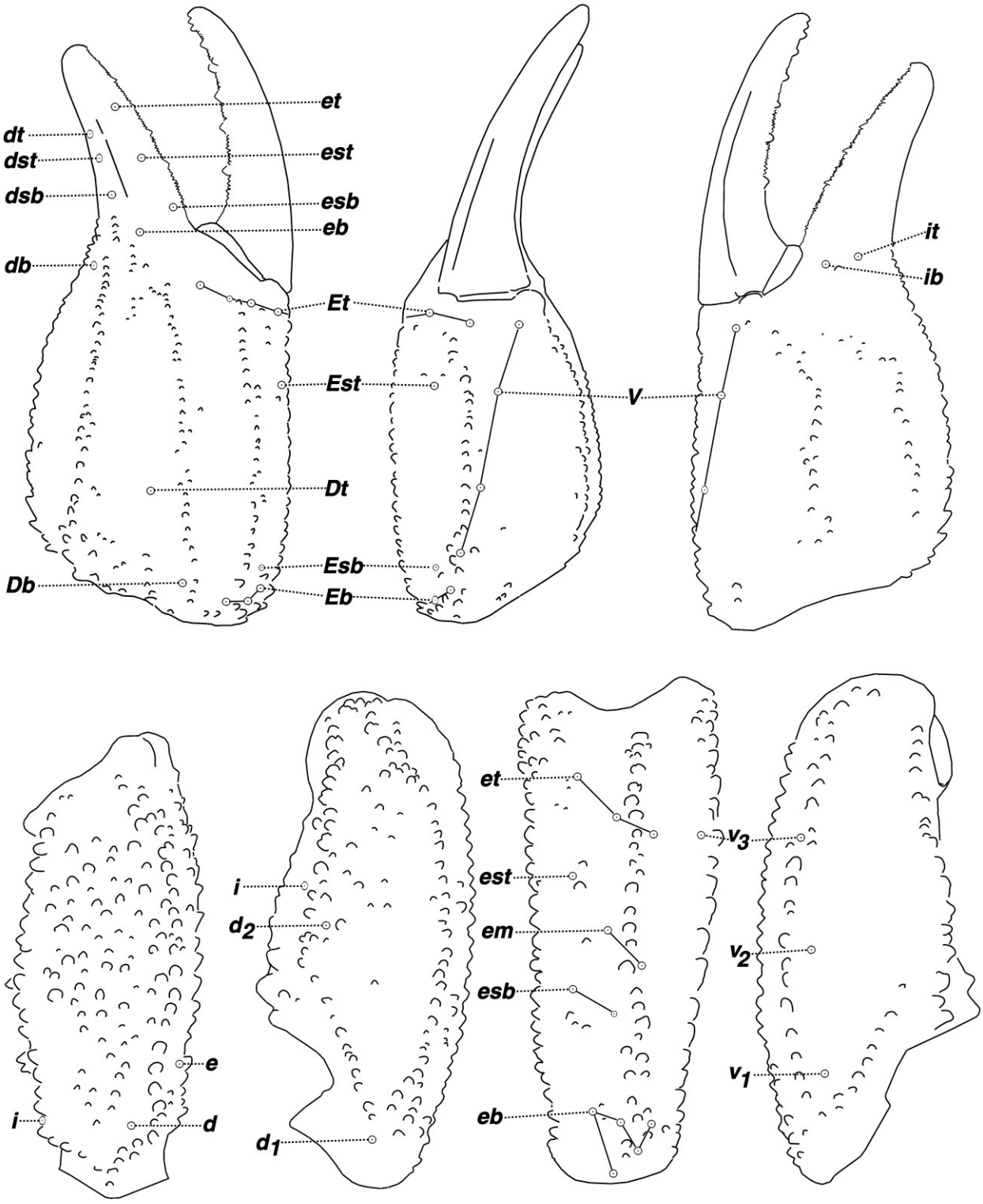

Figure 13: *Pseudouroctonus santarita*, **sp. nov**., paratype male. Trichobothrial pattern.

and ventrointernal carinae heavily serrated, dorsoexternal crenulated, and ventroexternal with scattered rounded granules. Dorsal and ventral surfaces scattered with granules, internal surface scattered with large granules, and external surface smooth. **Patella:** Dorsointernal, ventrointernal, dorsoexternal and ventroexter-

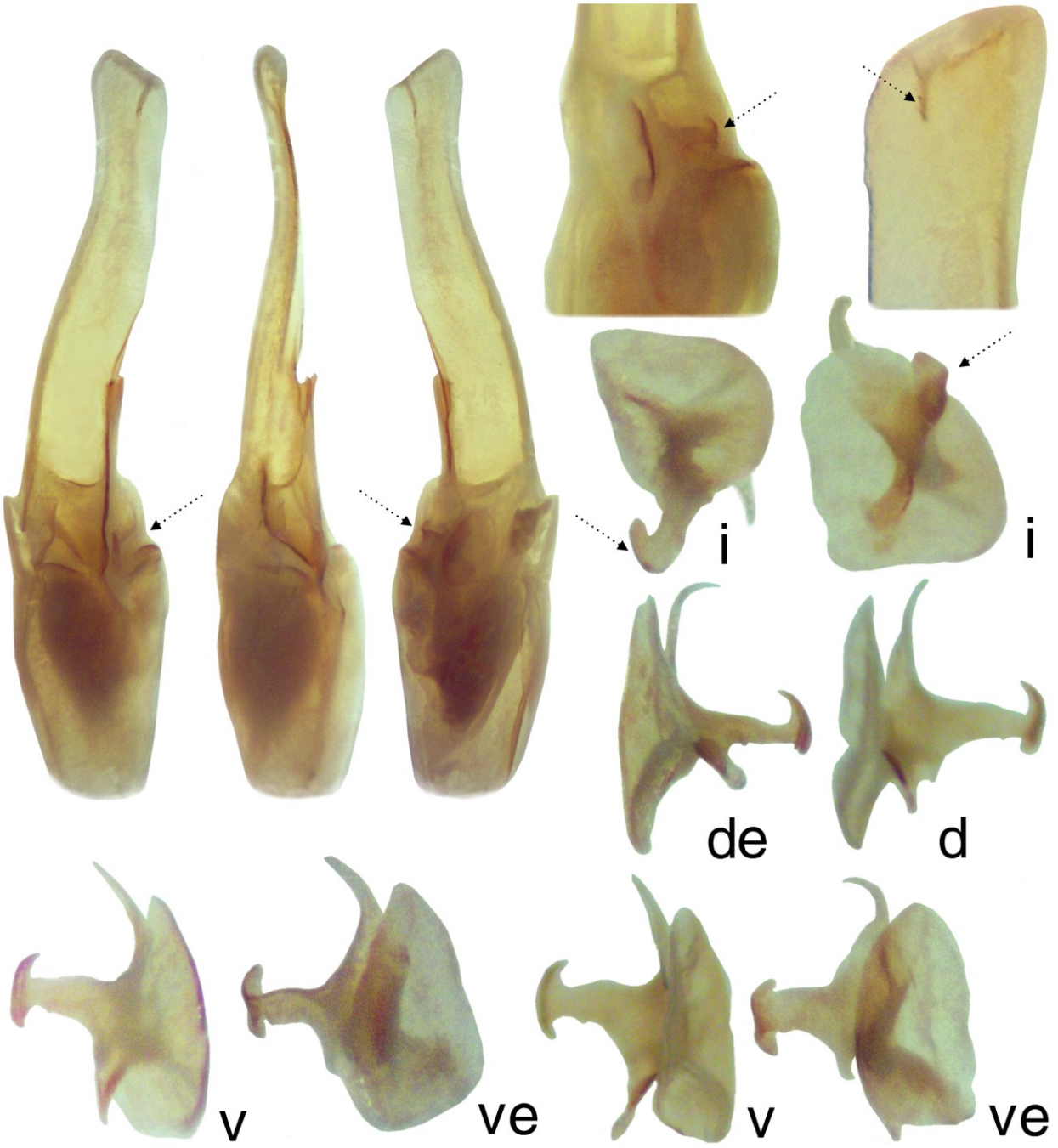

Figure 14: *Pseudouroctonus santarita*, **sp. nov**., male paratype, Madera Canyon, Santa Rita Mountains, Pima Co., Arizona, USA. Hemispermatophore and mating plug (photographed submerged in alcohol). **Upper-Left.** Right hemispermatophore, dorsointernal, exterodorsal, and ventral views. Arrows indicate partially visible embedded mating plug in dorsal and ventral views. **Upper-Right.** Left hemispermatophore, closeup of median area, ventrointernal view, showing embedded mating plug (arrow points to barb); and dorsal view of lamina terminus showing distal crest (pointed to by arrow). **Right.** Extracted left mating plug (reversed), two internal, dorsoexternal, dorsal, ventral, and ventroexternal views (arrows point to barb). **Lower-Left.** Extracted right mating plug, ventral and ventroexternal views. i = internal, de = dorsoexternal, d = dorsal, v = ventral, and ve = ventroexternal.

nal carinae heavily serrated, and exteromedian carina singular, strong and crenulated. Dorsal surface with slight scattering of granules, and ventral rough but with no granulation; external surface with serrated extero-median carina and 2–3 small granules in promity of trichobothrium *et*; internal surface smooth with medium sized DPS and small VPS. **Chelal carinae:** Complies to the "10-carinae configuration". Digital (*D1*) carina

Figure 15: *Pseudouroctonus santarita*, **sp. nov**., Madera Canyon, Santa Rita Mtns., Pima Co., Arizona, USA. **Top.** Paratype juvenile in natural habitat. **Bottom.** Paratype female with first instar juveniles.

Figure 16: *Pseudouroctonus santarita*, **sp. nov**., Madera Canyon, Santa Rita Mtns., Pima Co., Arizona, USA. **Top.** Habitat. **Bottom.** Microhabitat.

strong and serrated; subdigital (*D2*) essentially obsolete, composed of two small granules; dorsosecondary (*D3*) flat with delicate granules; dorsomarginal (*D4*) medium to strong with scattered granulation; dorsointernal (*D5*) medium with large granules; ventroexternal (*V1*) strong and serrated, terminating at external condyle of movable finger; ventromedian (*V2*) essentially obsolete; ventrointernal (*V3*) strong with scattered granulation; external (*E*) medium with small granules. **Chelal finger dentition (Fig. 10):** Median denticle (*MD*) row groups aligned in a straight line, 6 on the fixed and movable fingers; 6/6 *ID*s on fixed finger and 7/7 *ID*s on movable finger; 5/5 *OD*s on fixed finger and 6/6 *OD*s on movable finger. No accessory denticles present. The number of *MD*s on the fixed finger for each row: right finger: *md1* = 5, *md2* = 6, *md3* = 7, *md4* = 7, *md5* = 8, *md6* = 15: total = 48; left finger: *md1* = 5, *md2* = 7, *md3* = 9, *md4* = 9, *md5* = 5, *md6* = 14: total = 49. **Trichobothrial patterns (Fig. 13):** Type C, orthobothriotaxic. Trichobothria *ib*-*it* located basally, *ib* on the palm and *it* on the fixed finger base; chelal V_4 is located on the *V1* carina; *Db* is located external to the *D1* carina; *Dt* is positioned well on the proximal half of the palm; patellar v_3 is located adjacent to et_3.

LEGS (Fig. 9). Both pedal spurs present on all legs, lacking spinelets; tibial spurs absent. Ventral surface of the tarsus with a median row of short spinules terminating distally with two pairs of spinules. Unguicular spine well-developed and pointed.

HEMISPERMATOPHORE (FIG. 14, paratype male). Lamina edges subparallel, terminus truncated with a subtle distal crest on the dorsal side (also visible from the ventral side due to the structure's translucency). Lamellar hook elongated, distinctly bifurcated, and originating from the dorsal trough. A secondary lamellar hook and basal constriction are absent. Left hemispermatophore length = 3.50 mm, lamina length = 2.40 mm, lamellar hook length = 0.95 mm, and trough difference = 0.44 mm. Right hemispermatophore lamina length = 2.40 mm, lamellar hook length = 0.90 mm, and trough difference = 0.45 mm. Lamellar hook length to lamina length ratio is 0.375 and trough difference to lamellar hook length ratio is 0.500. Mating plug with a smooth barb, its distal edges essentially straight, thus not "crescent-shaped". At the base of the plug a conspicuous projection extends from the brace-A substructure, beyond the base edge. A smaller projection also extends from brace-B. Above the brace-B projection, there is a small projection extending from the stock.

Male and female variability. There is no significant sexual dimorphism involving morphometrics. Though the male has a slightly thinner metasoma in segments II–V, the MVDs (L/W) only range from 3.1 to 6.3 %. The chela fixed finger is also shorter in the male when compared to the metasomal segment lengths, in particular segments II–V, exhibiting MVDs ranging from 9.5 to 12.9 %. Pectinal tooth counts in males exceed those of females by 2 teeth, male 10–12 (11.000) [14], female 8–10 (9.000) [29]. The genital operculum sclerites are fused medially except for the posterior one-third in the female, whereas they are separated along their entire length in the male, exposing developed genital papillae. See Appendix B for more statistical-based information.

Reproduction. Several females were kept alive in captivity in order to observe them giving birth and to count the number of 1st instar juveniles. As can be seen in Figure 15, the 1st instar behavior is similar to scorpions in the genus *Vaejovis*, recently reported by Ayrey (2013a). The 1st instar orientation on the mother's back is non-random, as is seen with many other species in the family Vaejovidae (Hjelle, 1974). They face anteriorly with the prosoma down and the metasoma raised over the prosoma of the juvenile immediately posterior to them, the same behavior as *V. halli* (Ayrey, 2012), *V. trinityae* (Ayrey, 2013b) and many other species of the "vorhiesi" group of the genus *Vaejovis* (Ayrey, 2013a). Postpartum behavior is as described in Ayrey (2013b). Although the specimen in Figure 15 does not, most of this species exhibit some random 1st instar behavior similar to *Pseudouroctonus kremani*, **sp. nov**.

The main difference in the reproduction of this species, and most of the Vaejovidae, is that they exhibit iteroparity. The author has been observed this several times. The female pictured in Figure 15 had young in August of 2008 and again in August of 2010, yet it was kept isolated from all other scorpions during the intervening years.

Pseudouroctonus kremani Ayrey et Soleglad, sp. nov.

(Figs. 17–32; Table 1)

http://zoobank.org/urn:lsid:zoobank.org:act:210F6F08-C6F9-49A9-986D-BCC95A8D8A58

REFERENCES:

Uroctonus apacheanus: Gertsch & Soleglad, 1972: 576, 577 (in part).

Pseudouroctonus apacheanus: Bryson et al., 2013: 5, 6, figs. 1, 2.

Type material. Holotype ♀, Seven Cataracts Overlook, Catalina Highway, Santa Catalina Mountains, Pima County, Arizona, USA (32.35202, -110.72495; 1601 m asl), 25 August 2014, leg. R.F. Ayrey (#RA1020, USNM); paratypes 2 ♀, same locality and date, (#1019, #1018 RFA); ♂, Molino Basin, Santa Catalina Mountains, Pima County, Arizona, USA, 19 August 2012, leg. R.F. Ayrey (#707, USNM), ♀, same locality, 19 October 2014, leg. R.F. Ayrey (#1074, RFA).

Diagnosis. Small species with heavy chelae, 25–34 mm. Pectinal tooth counts 11–12 males, 9–10 females; meta-

Figure 17: *Pseudouroctonus kremani*, **sp. nov.,** Santa Catalina Mtns., Pima Co., Arizona, USA. **Top.** Holotype female in natural habitat. **Bottom.** Paratype subadult female.

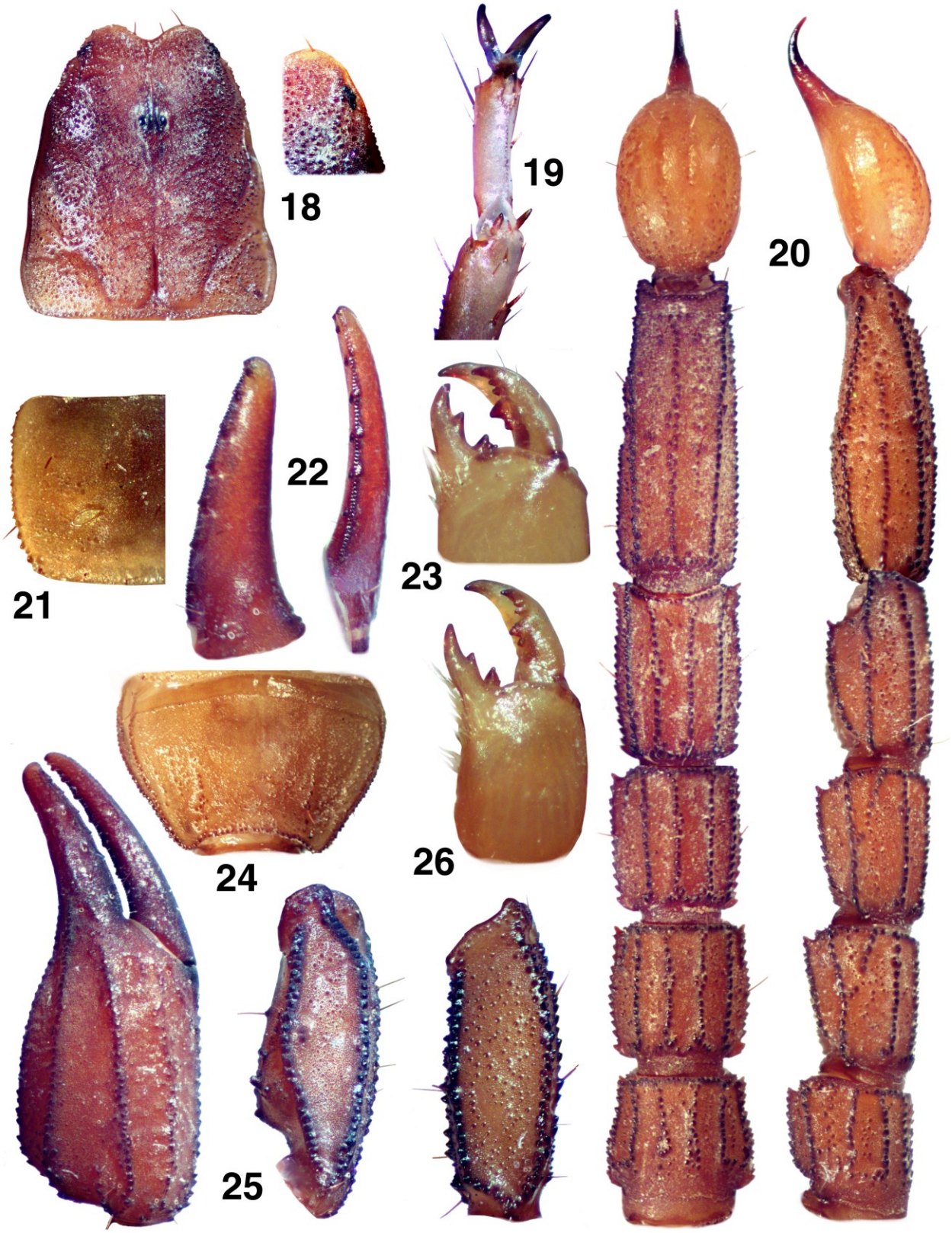

Figures 18–26: *Pseudouroctonus kremani*, **sp. nov**. **Figs. 18–25.** Holotype female. **Fig. 26.** Paratype male. **18.** Carapace and closeup of left lateral eyes. **19.** Right leg III, ventral view. **20.** Metasoma and telson, ventral and lateral views. **21.** Right stigma III. **22.** Fixed and movable finger dentition. **23.** Chelicera, dorsal view, showing smooth ventral edge. **24.** Sternite VII. **25.** Right chela, patella and femur. **26.** Chelicera, dorsal view, showing smooth ventral edge.

Figure 27: *Pseudouroctonus kremani*, **sp. nov**. Sternopectinal area of paratype female (left) and paratype male (right).

soma relatively thin, segments III–V length to width ratio 1.06–1.09, 1.41–1.41, and 2.40–2.41 in males, 1.08, 1.39, and 2.35–2.50 in females; metasomal segments IV–V widths to fixed finger length ratio 0.71–0.77 and 0.67–0.73 in males, 0.60–0.63 and 0.57–0.60 in females; fixed finger *MD* counts 51–54 for males and 57–62 for females; hemispermatophore lacking distal crest on lamina terminus; mating plug lacking projections on brace-A and brace-B.

Distribution. Santa Catalina Mountains, southern Arizona, USA. See map in Fig. 33.

Etymology. This species is named in honor of Michael Kreman who provided invaluable assistance with the photography.

FEMALE. The following description is based on holotype female from the Santa Catalina Mountains, Arizona, USA. Measurements of the holotype female and paratype male are presented in Table 1. See Figure 17 for photographs of live holotype and paratype female specimens.

COLORATION. The posterior half of the carapace and mesosoma orange-brown; carapace anterior half brown. Metasoma brown with darker carinae; telson vesicle light brown. Pedipalps brown with darker carinae. Sternopectinal area and sternites light brown; legs brown.

CARAPACE (Fig. 18). Anterior edge with a conspicuous narrow median indentation, providing a ratio of 0.058 when its depth is compared to the carapace's length; edge with five setae visible (one missing); entire surface densely covered with medium sized granules. Three lateral eyes are present, the posterior eye considerably smaller. Median eyes and tubercle of medium size, positioned anterior of middle with the following length and width ratios: 0.331 (anterior edge to medium tubercle middle / carapace length) and 0.138 (width of median tubercle including eyes / width of carapace at that point).

MESOSOMA (Figs. 21, 24). Tergites I–VII densely covered with small granules; tergite VII lateral and median carinae strong and crenulate. Sternites III–VI smooth, VII with small dense granules on posterior lateral aspects; sternite VII with irregularly granulated lateral carinae and obsolete median carinae (Fig. 24). Stigmata (Fig. 21) are small to medium in size and elliptical in shape.

METASOMA (Fig. 20). Segment I–II wider than long. Segments I–IV: dorsal and dorsolateral carinae serrated; dorsal and dorsolateral (I–III) carinae terminate with an enlarged spine; lateral carinae serrated on I, serrated on posterior one-third of II and III, oboslete on segment IV; ventrolateral and ventromedian carinae serrated. Dorsolateral carinae of segment IV terminate essentially at the articulation condyle. Segment V: dorsolateral carinae serrated; lateral carinae serrated for two-thirds of posterior aspect; ventrolateral and single ventromedian carinae serrated; ventromedian carina not bifurcated, terminating in straight line. Anal arch with 15 small granules. Intercarinal areas of segments I–V scattered with minute granules.

TELSON (Fig. 20). Vesicle fairly robust with well defined granules located on the ventral surface; mod-

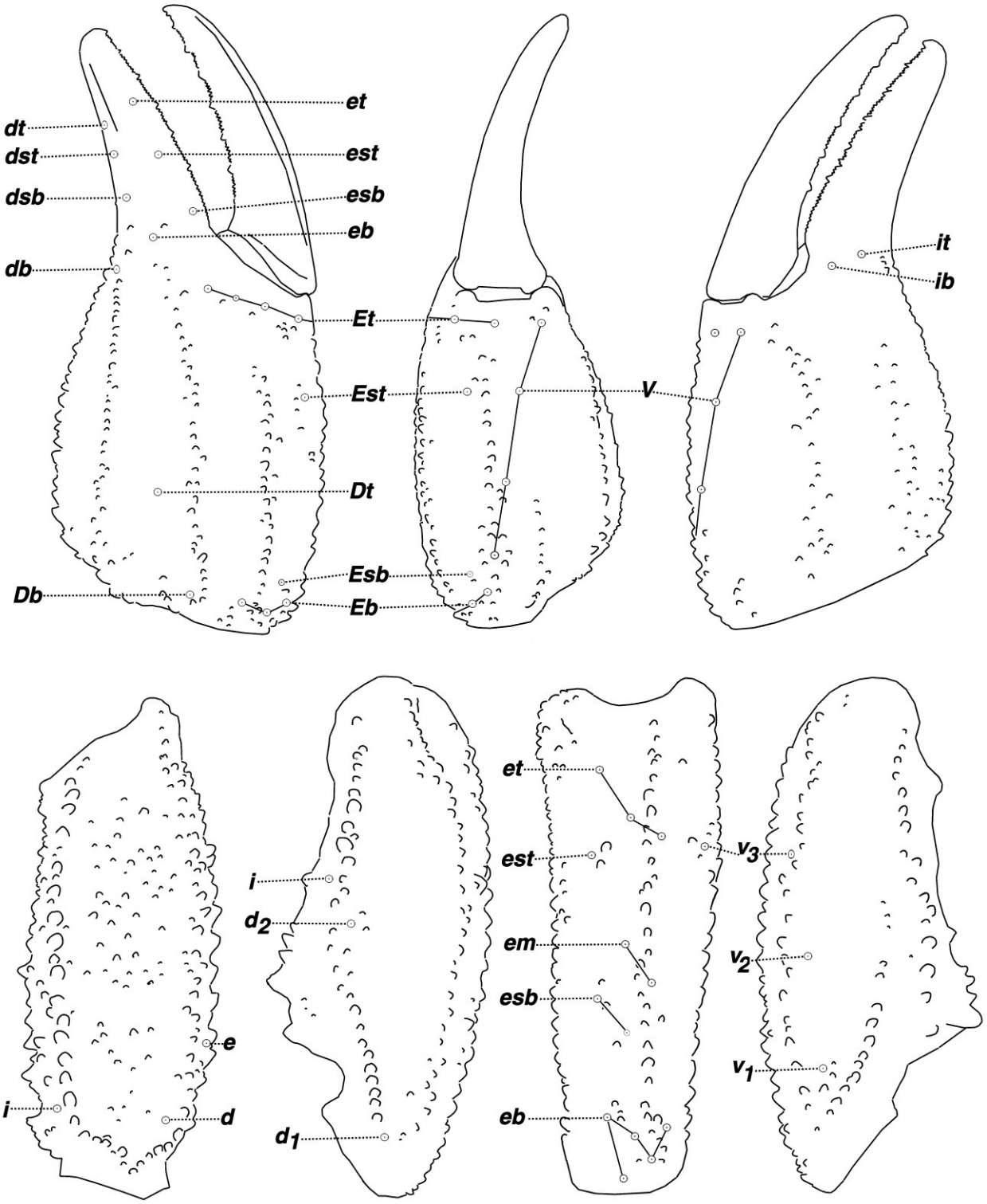

Figure 28: *Pseudouroctonus kremani*, **sp. nov**., paratype male. Trichobothrial pattern.

erate setation on ventral surface. Aculeus with medium curve, well delineated from the vesicle when viewed ventrally. Vesicular tabs with a single small curved spine.

PECTINES (Fig. 27, paratype male). Well-developed segments exhibiting length / width ratio 2.821 (length taken at anterior lamellae / width at widest point including teeth). Sclerite construction complex, three anterior

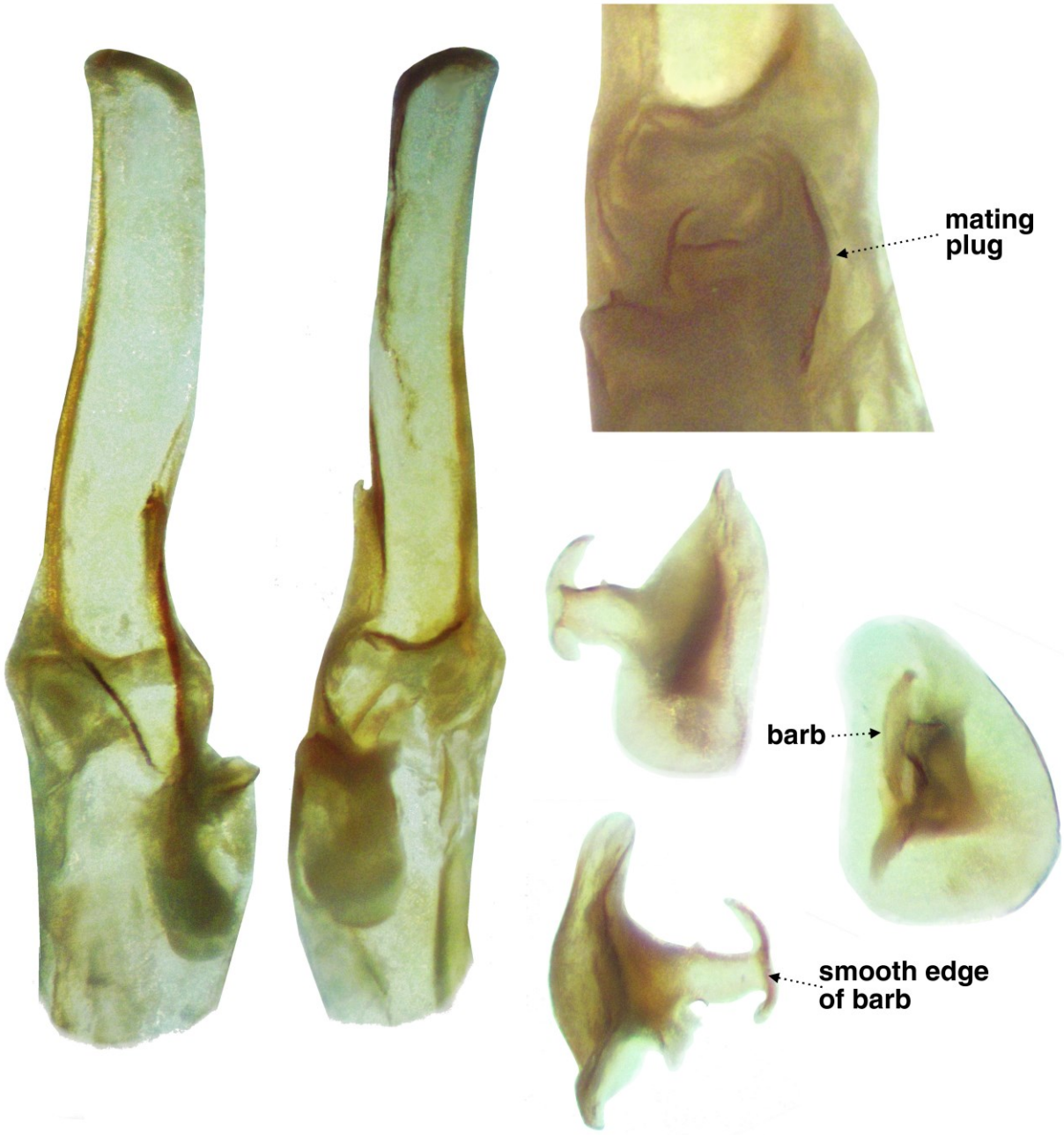

Figure 29: *Pseudouroctonus kremani*, **sp. nov**. Right hemispermatophore and mating plug (photographed submerged in alcohol). **Left.** Complete hemispermatophore, dorsal and ventral views (note, the terminal area of the trunk is missing). **Upper-Right.** Closeup of ventral median area showing an embedded mating plug. **Lower-Right.** Extracted mating plug, ventral, dorsal, and interoventral views (far right).

lamellae and six middle lamella; fulcra of medium development. Teeth number 9/9. Sensory areas developed along most of tooth inner length on all teeth, including basal tooth. Scattered setae found on anterior lamellae and distal pectinal tooth. Basal piece large, with well developed wide indentation along anterior edge, length / width ratio 0.519.

GENITAL OPERCULUM (Fig. 27). Sclerites triangular, wider than long, separated on posterior one-third.

STERNUM (Fig. 27). Type 2, posterior emargination present, well-defined convex lateral lobes, apex shallow; sclerite wider than long, in ratio 0.880.

CHELICERAE (Figs. 23. 26). Movable finger dorsal edge with two subdistal (*sd*) denticles; ventral edge smooth with well developed serrula on distal half (with 20+ tines). Ventral distal denticle (*vd*) slightly longer than dorsal (*dd*). Fixed finger with four denticles, median (*m*) and basal (*b*) denticles conjoined on common trunk; no ventral accessory denticles present.

Figure 30: *Pseudouroctonus kremani*, **sp. nov.,** Santa Catalina Mtns., Pima Co., Arizona, USA. **Top.** Female with first instar juveniles. **Bottom.** Female with second instar juveniles.

Figure 31: *Pseudouroctonus kremani*, **sp. nov.,** Santa Catalina Mtns., Pima Co., Arizona, USA. Gravid paratype female.

PEDIPALPS (Figs. 25, 22, 28). Well-developed chelae, with medium lengthed fingers, carinae well developed, no scalloping on the fingers. Planes formed by carinae *D1|D3|D4* and *V1|V2|V3* are essentially parallel. **Femur:** Dorsointernal and ventrointernal carinae heavily serrated, dorsoexternal crenulated, and ventroexternal with scattered rounded granules. Dorsal and ventral surfaces scattered with granules, internal surface scattered with large granules, and external surface smooth. **Patella:** Dorsointernal, ventrointernal, dorsoexternal and ventroexternal carinae heavily serrated, and exteromedian carina singular, strong and crenulated. Dorsal surface with minute scattered granules, and ventral rough but with no granulation; external surface with serrated exteromedian carina and 2–3 small granules in promity of trichobothrium *et* plus a few scattered granules continuing to the base of the segment; internal surface smooth with medium sized DPS and small VPS. **Chelal carinae:** Complies to the "10-carinae configuration". Digital (*D1*) carina strong and serrated; subdigital (*D2*) essentially obsolete, composed of four small granules; dorsosecondary (*D3*) flat with delicate granules; dorsomarginal (*D4*) medium to strong with scattered granulation; dorsointernal (*D5*) medium with large granules; ventroexternal (*V1*) strong and serrated, terminating at external condyle of movable finger; ventromedian (*V2*) essentially obsolete with some scattered granules on basal area; ventrointernal (*V3*) strong with scattered granulation; external (*E*) medium with small granules. **Chelal finger dentition (Fig. 22):** Median denticle (*MD*) row groups aligned in a straight line, 6 on the fixed and movable fingers; 6/6 *ID*s on fixed finger and 7/7 *ID*s on movable finger; 5/5 *OD*s on fixed finger and 6/6 *OD*s on movable finger. No accessory denticles present. The number of *MD*s on the fixed finger for each row: right finger: right: *md1* = 7, *md2* = 8, *md3* = 9, *md4* = 8, *md5* = 9, *md6* = 21: total = 62; left finger: *md1* = 7, *md2* = 7, *md3* = 8, *md4* = 10, *md5* = 9, *md6* = 19: total = 60. **Trichobothrial patterns (Fig. 28):** Type C, orthobothriotaxic. Trichobothria *ib*-*it* located basally, *ib* on the palm and *it* on the fixed finger base; chelal V_4 is located on the *V1* carina; *Db* is located external to the *D1* carina; *Dt* is positioned well on the proximal half of the palm; patellar v_3 is located slightly basal to et_3.

LEGS (Fig. 19). Both pedal spurs present on all legs, lacking spinelets; tibial spurs absent. Ventral surface of the tarsus with a median row of short spinules terminating distally with two pairs of spinules. Unguicular spine well-developed and pointed.

HEMISPERMATOPHORE (Fig. 29, paratype male). Lamina edges subparallel, terminus truncated, lacking a distal crest on the dorsal side. Lamellar hook elongated,

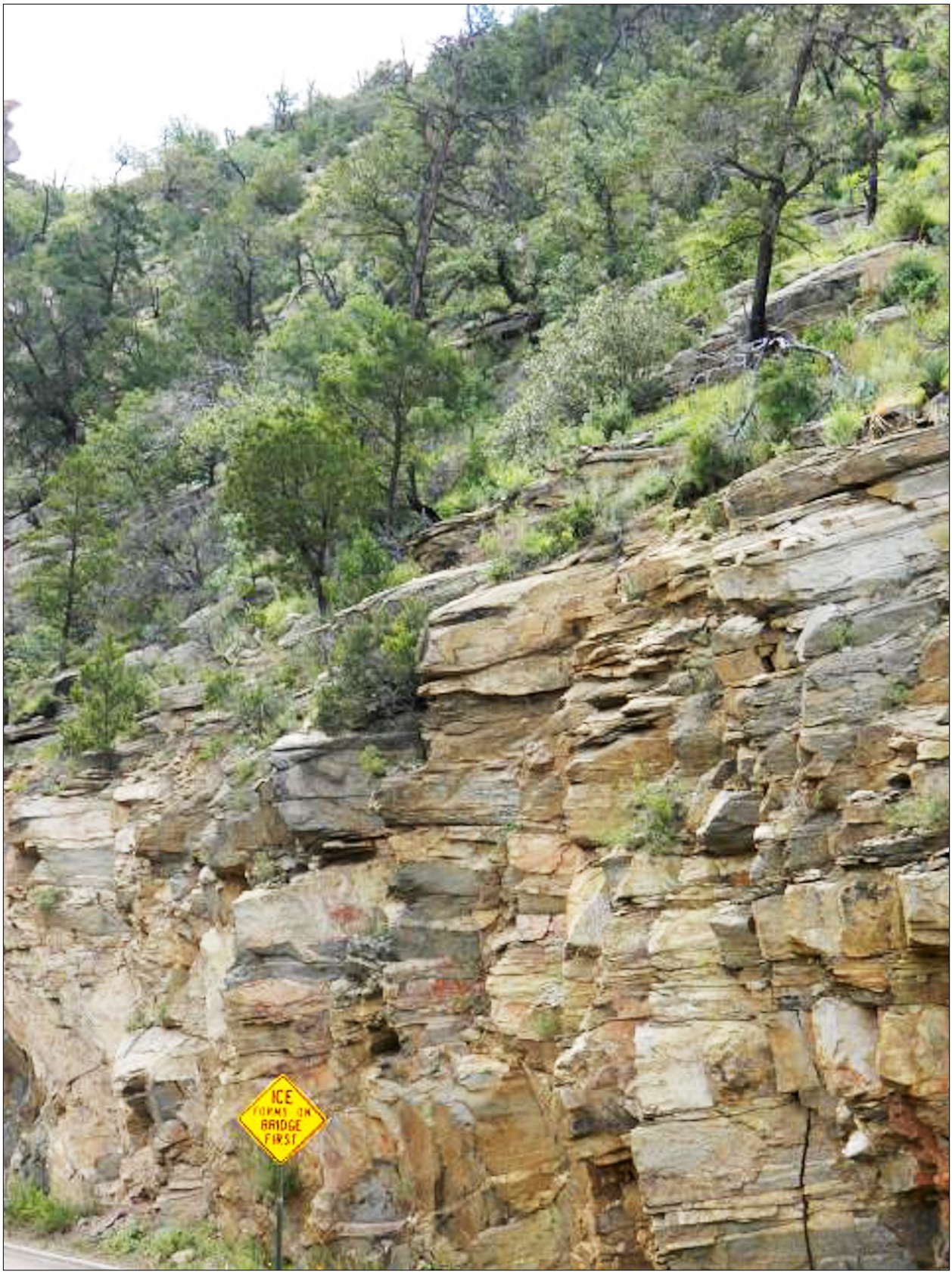

Figure 32: *Pseudouroctonus kremani*, **sp. nov.,** Santa Catalina Mtns., Pima Co., Arizona, USA. Habitat.

	P. kremani, sp. nov.		*P. santarita*, sp. nov.		*P. apacheanus*	
	Female Holotype	**Male Paratype**	**Female Holotype**	**Male Paratype**	**Female Topotype**	**Male Topotype**
Total length	32.40	24.85	28.50	24.10	27.25	27.15
Carapace length	4.50	3.55	3.95	3.35	3.80	3.90
Mesosoma length	11.50	7.00	9.60	6.50	8.50	7.70
Metasoma length	12.30	10.80	11.25	10.75	11.15	11.60
Segment I length/width	1.65/2.05	1.50/1.85	1.50/2.10	1.30/2.00	1.40/2.05	1.50/2.15
Segment II length/width	1.90/1.95	1.60/1.70	1.70/2.10	1.70/1.95	1.70/2.00	1.75/2.15
Segment III length/width	2.00/1.85	1.85/1.70	1.85/2.05	1.80/1.90	1.85/2.00	1.90/2.10
Segment IV length/width	2.50/1.80	2.25/1.60	2.30/1.95	2.25/1.85	2.30/1.90	2.45/1.90
Segment V length/width	4.25/1.70	3.60/1.50	3.90/1.90	3.70/1.70	3.90/1.80	4.00/1.90
Telson length	4.10	3.50	3.70	3.50	3.80	3.95
Vesicle length	2.70	2.30	2.40	2.30	2.50	2.60
width/depth	1.75/1.40	1.40/1.10	1.60/1.25	1.40/1.10	1.60/1.30	1.60/1.30
Aculeus length	1.40	1.20	1.30	1.20	1.30	1.35
Pedipalp length	14.75	11.60	12.25	11.00	12.80	12.85
Femur length/width	3.60/1.30	2.80/1.10	3.00/1.30	2.60/1.10	3.30/1.20	3.20/1.30
Patella length/width	4.00/1.55	3.10/1.35	3.30/1.55	3.00/1.30	3.40/1.40	3.40/1.50
Chela length	7.15	5.70	5.95	5.40	6.10	6.25
Palm length	3.80	3.10	3.25	3.00	3.10	3.30
width/depth	2.20/2.80	1.85/2.50	2.10/2.65	1.95/2.40	1.95/2.45	2.20/2.80
Fixed finger length	2.85	2.25	2.30	2.00	2.55	2.50
Movable finger length	4.00	3.10	3.25	2.85	3.45	3.50
Pectines						
teeth	9-9	11-11	9-9	11-10	10-10	11-12
middle lamellae	5-5	5-5	6-6	7-7	6-6	7-6
Sternum length/width	1.10/1.25	0.95/1.05	1.00/1.20	0.90/1.10	1.10/1.25	1.00/1.10

Table 1: Morphometrics (mm) of three *Pseudouroctonus* species from southern Arizona. *P. kremani*, **sp. nov.,** Santa Catalina Mountains, Pima Co., Arizona, USA, *P. santarita*, **sp. nov.,** Madera Canyon, Santa Rita Mountains, Pima Co., Arizona, USA, and *P. apacheanus*, Rucker Canyon, Chiricahua Mountains, Cochise County, Arizona, USA.

distinctly bifurcated, and originating from the dorsal trough. A secondary lamellar hook and basal constriction are absent. Right hemispermatophore lamina length is 2.50 mm, lamellar hook length = 1.00 mm., and trough difference = 0.50 mm. Lamellar hook length to lamina length ratio is 0.350 and trough difference to lamellar hook length ratio is 0.500. Mating plug with a smooth barb, its distal edges essentially straight, thus not "crescent-shaped". Projections from the brace-A and brace-B not present. Above the brace-B, there is a medium sized projection extending from the stock.

Male and female variability. The fixed finger is relatively longer in the female than in the male when its length is compared to the length and width of the five metasomal segments, exhibiting large MVDs ranging from 15.9–24.3 (20.56) %. In line with the longer fixed finger in the female, we see it also has a larger number of *MD* denticles, averaging 7.4 more denticles than that found in the male. The *MD* ranges, female 57–62 (59.667) [6], and male 51–54 (52.250 [4]. Interestingly, the metasoma ratios between the two sexes are essentially the same, when the segment length is compared to its width. Pectinal tooth counts in males exceed those of females by approximately 1.75 teeth, male 11–12 (11.214) [14], female 9–10 (9.469) [32]. The genital operculum sclerites are fused medially except for the posterior one-third in the female, whereas they are sep-

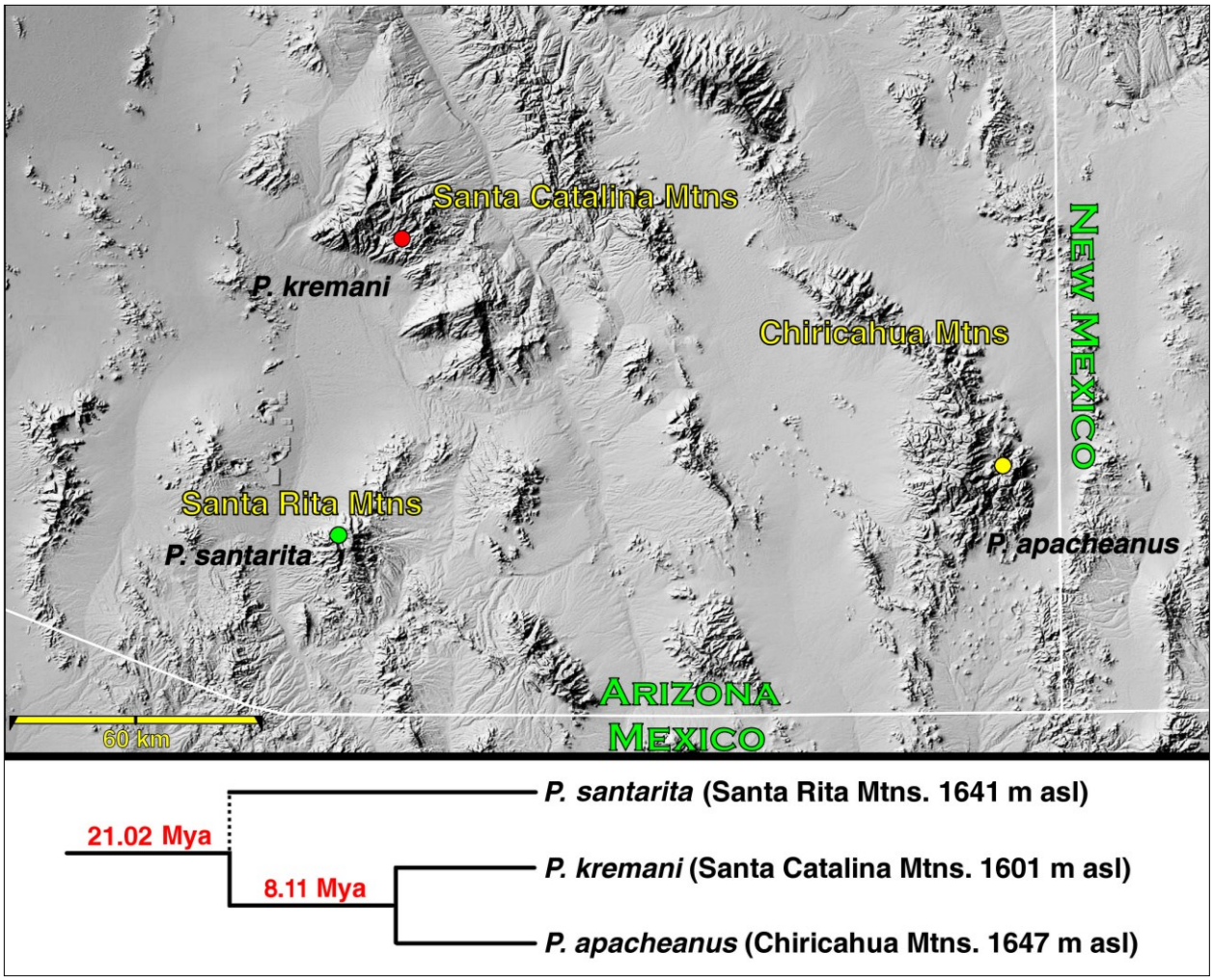

Figure 33: Proposed geographic and molecular relationships of three southeastern Arizona *Pseudouroctonus* species, *P. kremani*, **sp. n.** (red icon), *P. santarita*, **sp. n.** (green icon), and *P. apacheanus* (yellow icon). **Top.** Close-up of southeastern Arizona showing the type localities of the three species and the mountain ranges in which they occur, Santa Catalina, Santa Rita, and Chiricahua Mountains, respectively. **Bottom.** A partial chronogram based on molecular data showing proposed phylogenetic relationships based on evolutionary time indicating estimates for a multilocus species tree (red numbers depict means). 95% highest posterior densities are shown for each node. Information is from Bryson et al. (2013: fig. 3). Altitude data is that of the type localities.

arated along their entire length in the male, exposing developed genital papillae. See Appendix B for more statistical-based information.

Reproduction. Two females were kept alive in captivity in order to observe them giving birth and to count the number of first instar juveniles (see Figure 30). Both females gave birth in September, 2014 with the juvenile counts 32 and 33. The 1st instar orientation on the mother's back was similar to the "non-random" distribution reported by Ayrey and Hjelle (Ayrey, 2009; Ayrey, 2011; Ayrey & Webber, 2013; Ayrey, 2014; Ayrey & Soleglad, 2014; and Hjelle, 1974). The main difference is that in most *Pseudouroctonus* females there are several 1st instars that are oriented randomly (see Figure 30). Postpartum behavior is similar to that described in Ayrey, 2013a.

Comparison of Species

The three southern Arizonan *Pseudouroctonus* species discussed in this contribution can be separated by comparisons of the hemispermatophore and its mating plug, the number of median denticles (*MD*) found on the chelal fixed finger, and several morphometric ratios. According to the suggested phylogeny of Bryson et al. (2013), a result of their molecular analysis (see chronogram in our Fig. 33), *P. santarita* is distinctly separated from the other two species, *P. kremani* and *P. apacheanus* which in turn form their own clade. Based

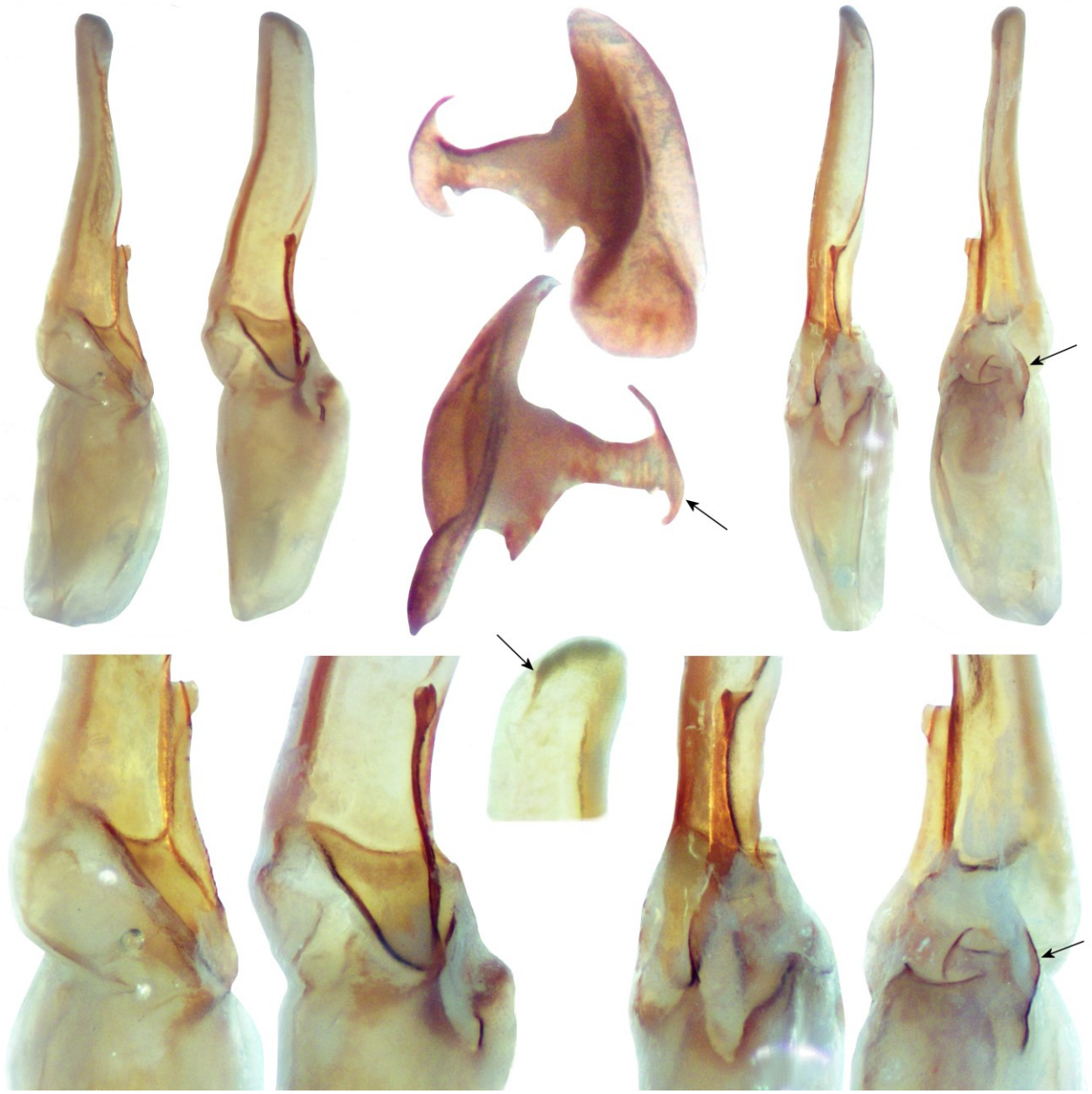

Figure 34: *Pseudourotonus apacheanus*, Rucker Canyon, Chiricahua Mountains, Cochise Co., Arizona, USA. Right hemispermatophore (photographed submerged in alcohol). **Upper Left.** Complete structure, exterodorsal and dorsal views. **Upper Right.** Complete structure, internal and interoventral views. **Lower.** Closeup of median area, exterodorsal, dorsal, internal, and interoventral views, showing the construction of the lamellar hook; and closeup of the lamina terminus of left hemisprmatophore showing the distal crest (arrow). **Upper Center.** Extracted mating plug, ventral and dorsal views, showing a smooth barb edge in the dorsal view (indicated by arrow). Note, the embedded mating plug in the median area is visible in the two interoventral views (indicated by arrows).

on these assumptions, we present the species comparisons in two parts, one separating *P. santarita* from the other two species, and the second comparision separating *P. kremani* from *P. apacheanus*, thus reflecting these suggested phylogenetic relationships.

Morphometric techniques. Based on a limited number of full adult measurement sets, male and female of each species, all morphometrics (26 in all, see Table 1) were digitized and analyzed as follows. 325 ratios (i.e., 26 morphometrics compared two at a time) were calculated against each species and both genders. Based on this initial analysis, key morphometrics were identified based on their dominance in the ratio comparison; i.e., they had the most affect on the comparisons. In this initial analysis, we encountered significant differences in the relative slenderness of the metasoma

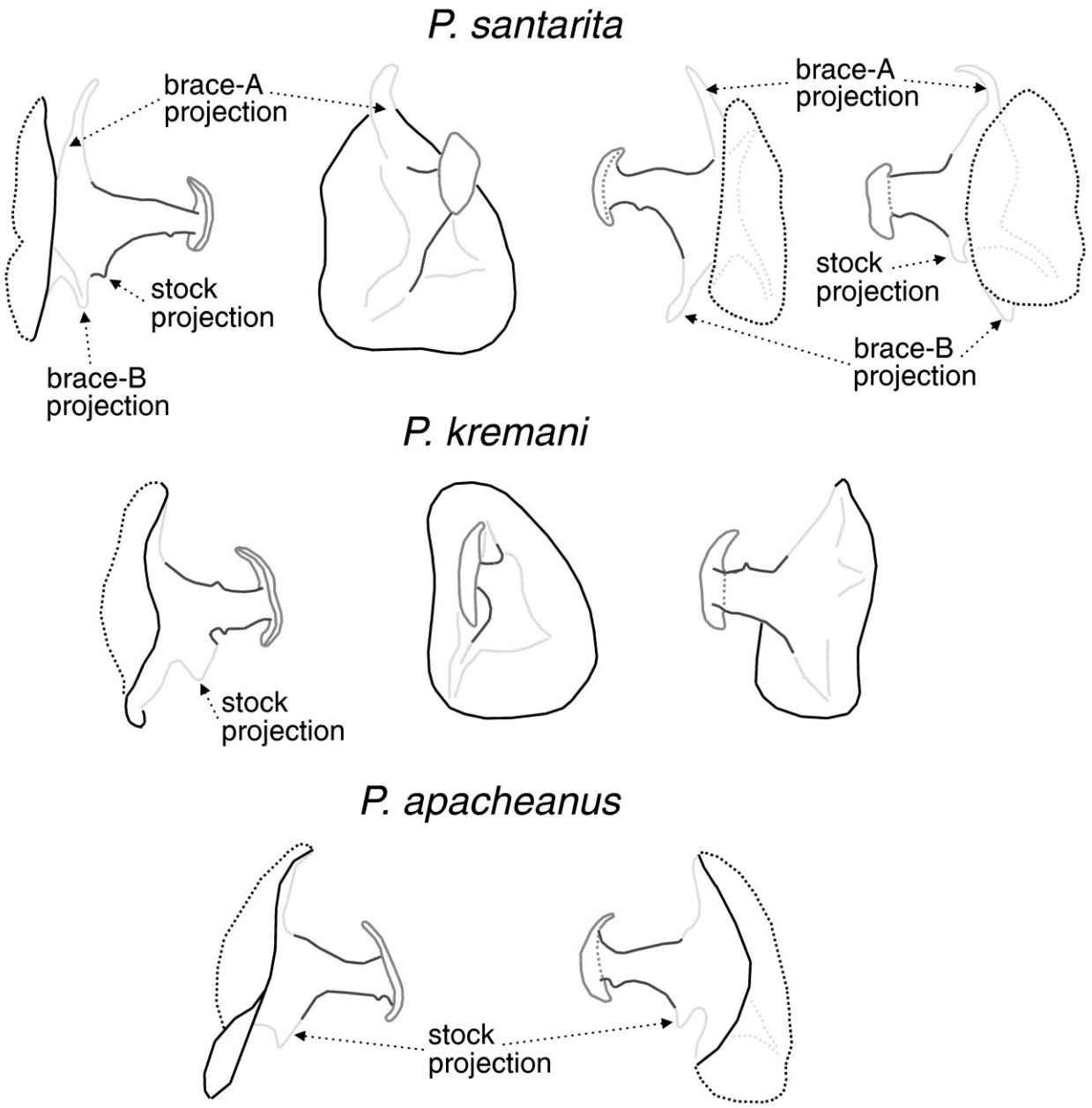

Figure 35: Diagrammatic views of the hemispermatophore mating plug for *Pseudouroctonus* species showing the brace and stock projections. **Top.** *P. santarita*, dorsal, internal, ventral, and ventroexternal views. **Middle.** *P. kremani*, dorsal, internal, and ventral views. **Bottom.** *P. apacheanus*, dorsal and ventroexternal views. The dotted lines indicate the following: barb edge showing through the stock in ventral views; braces showing through the base in ventral views; and the base edges visible from the external view.

and differences in the length of the chelal fingers. Based on this, other measurements, specifically the metasoma length and width, and lengths of the fixed and movable fingers, were obtained from other male and female specimens thus expanding our sample set.

Each species was then compared against the other two species, for each sex, and the two sexes per species were also compared to each other. As we discuss in detail below, we encountered morphometric ratio differences significant enough to consider them diagnostic. The final results of the morphometric analysis verified that the metasoma and fixed and movable fingers provided the best diagnostic characters, this involving eighteen adult specimens. See Appendix B for all statistical results.

Chelal fixed finger *MD* counts. Based on the diagnostic-level observations of the chelal finger morphometric analysis, in particular the fixed finger, we

decided to count the number of *MD* denticles on this finger. The assumption here is, since these species are closely related and very similar in there overall morphology, the *MD* denticles would be constructed the same as far as shape, size, spacing, etc. are concerned. Therefore, we suspected species with shorter fingers would also have a smaller number *MD* denticles. By the way, it is important that these three species are closely related, because Soleglad & Fet (2006: 12–13; tabs. 1–2) demonstrated that not all chelal finger dentition is constructed the same in shape, size, or spacing. This was especially apparent for the unusal vaejovid tribe Stahnkeini whose *MD* denticles are highly serrated, flattened in a lateral perspective, thus wider on the finger edge, resulting in a smaller number of denticles. In the author's table 2 we see, after normalized to the scorpion's adult size and finger length, that the genera *Pseudouroctonus* and *Uroctonites* have more than twice as many *MD* denticles on the movable finger than that found in tribe Stahnkeini.

Our suspicions above were, of course, confirmed: the species with the shortest fixed finger of the three considered in this paper did indeed exhibit the smallest number of *MD* denticles. In Appendix B we present all statistical data involving the number of *MD* denticles tabulated for the fixed finger. The denticle counts are divided into the six *MD* denticle rows occurring on this finger, each row is tabulated separately. In all, 36 fixed fingers were tabulated.

P. santarita

The primary diagnostic morphology that distinguishes *P. santarita* from the other two species is its relatively complex structure of the hemispermatophore mating plug, its proportionally short chelal fixed finger, and a smaller number of *MD* denticles on this finger, a character further endorsing its short fingers.

Hemispermatophore and Mating Plug. In this paper we identified additional substructures for the vaejovid mating plug. In Figure 2 three stock braces (brace-A, -B, and -C) were identified, substructures that support the stock's attachment to the mating plug's base. In general these braces are low-profile in nature as situated on the base, slightly sclerotized, and only visible in certain views.

Figure 34 shows diagrammatic views of all three species contrasted in this paper. For *P. santarita*, whose mating plug is the most complex of the three, we provide four separate views, the dorsal, internal, ventral, and ventroexternal views. In these views we see two conspicuous projections extending from brace-A and brace-B, the former the most visible since it extends beyond the base's edge and is visible from all four views. These projections are not connected to the base as the braces are, but instead are raised slightly from the brace's surface. Above brace-B (that is, towards the barb), a small projection extends from the stock. In the other two *Pseudouroctonus* species, the two brace projections are absent and the stock projection is somewhat larger than that seen in *P. santarita*.

We consider these brace projections exhibited in *P. santarita* important diagnostic characters for this species. In all mating plugs available across these three species (eight in all, see Appendix B), we see consistency in these characters as illustrated in Figure 34. Now, whether the two brace projections are derived in *P. santarita* or pleisomorphic remains to be determined. Cladistic analysis of this interesting group of vaejovids, including genus *Uroctonites*, is presently underway. The problem here is very few hemispermatophore mating plugs have been adequately described and/or illustrated, if at all. The mating plug was described and illustrated for two species of *Kovarikia* by Soleglad, Fet & Graham (2014: 3–6; figs. 2–3, A-4) which proved to be diagnostic, including the hemispermatophore. Tate et al. (2013: fig. 17) also illustrated the mating plug for *P. peccatum*.

Finally, *P. santarita*'s hemispermatophore has a distal crest on its lamina terminus. This was verified in all six hemispermatophores examined. In the other two species, its occurrence is variable, depending on the species (see discussion below).

Fixed finger *MD* denticles. During the morphometric analysis of these three species, which included the generation of all possible morphometric ratios (technique described above), we detected differences in the length of the chelal fingers, in particular the fixed finger. As discussed above, based on this observation we decided to tabulate the number of *MD* denticles on the fixed finger, a potential diagnostic character.

P. santarita has relatively the shortest fixed fingers of the three species discussed in this paper. The morphometric differences, discussed below, definitely establish this fact. We calculated the number of *MD* denticles on the fixed finger on a row by row basis, with the possibility seeing a trend in one row or the other. This was tabulated on 36 fixed fingers of the three species in consideration.

The number of *MD* denticles on the fixed finger of *P. santarita* is definitely less than that found on the other two species. The ranges of the three species is 46–50 (48.667) [6] for *P. santarita* males and 47–53 (49.375) (±2.134) [8] females as compared to 60–72 (65.167) (±4.622) [6] for *P. apacheanus* males and 61–68 (64.500) (±2.258) [6] females, and 51–54 (52.250) (±1.258) [4] for *P. kremani* males and 57–62 (59.667) (±1.751) [6] females. The MVD comparisons between *P. santarita* and the other two species, including both genders, is shown in Appendix B, ranging from 7.4 to 33.9 percent, averaging 18.2 percent.

As far as *MD* denticle counts in the individual rows found on the fixed finger (i.e., six in number), we see relative consistency across the three species with respect to which row has the most or least denticles. In general the row with the least *MD* denticles predictably is row-1, the most distal on the finger, ranging 4–8 denticles across the three species and the two genders. The denticle row with the largest number of denticles is, again predictable, row-6, which is the basal row. It ranges 13–23 denticles across species and their sexes.

Finally, the difference in *MD* denticle counts occurring between *P. kremani* sexes is interesting, noticeably larger in the female. In the other two species, the counts between genders are essentially the same. This interesting observation will be discussed and explained below.

Fixed finger morphometrics. As stated above, the chelal fixed finger of *P. santarita* is relatively shorter than it is in the other two species. In particular, based on the morphometric analysis techniques described above, this diagnostic character is the most observable when the fixed finger length is compared to the metasoma segments, both its lengths and widths. In the final analysis, it was clear that metasomal segment widths compared to the fixed finger length provided the most conspicuous differences.

In Appendix B we present a histogram in Figure B-2 showing results for both sexes when the metasomal segment widths (all five segments) are compared to the chelal fixed finger length. It is clear from the histogram that *P. santarita* has by far the shortest chelal fixed finger, exhibiting complete separation in the absolute ranges of the data for all five segments for both sexes. MVD comparisons for each species by gender is as follows: *P. apacheanus*: 14.7–17.6 % for males, 12.7–16.1 % for females; *P. kremani*: 15.9–20.9 % for males, 30.1–39.7 % for females. Again, we see the significantly large MVDs between the females of *P. santarita* and *P. kremani* as compared to those exhibited when the males are compared. The reasons for this will be discussed below.

P. kremani vs. P. apacheanus

It was established above *P. santarita* can be separated from these two species by the presence of projections from brace-A and brace-B of the mating plug, shorter chelal fixed fingers, and a smaller number of *MD* denticles on the fixed finger. Diagnostic characters separating species *P. kremani* from *P. apacheanus* include the hemispermatophore and metasoma morphometrics.

Hemispermatophore and Mating Plug. As stated above, both *P. kremani* and *P. apacheanus* lack projections on the mating plug brace-A and brace-B (see Figure 34). However, *P. kremani* lacks a distal crest on the hemispermatophore lamina terminus, whereas it is present on *P. apacheanus*. See Figures 14, 29, and 34. This was verified on four hemispermatophores for each species. It appears that the absence of the distal crest in *P. kremani* is derived since it occurs in *P. santarita*.

Metasoma morphometrics. *P. kremani* has the thinnest metasoma of the three species discussed in this paper. In Figure B-1 (i.e., Appendix B) we show a histogram comparing the five metasomal segment lengths to its width for all three species, both sexes. *P. kremani* clearly exhibited relatively thinner segments on all five, showing complete separation of standard deviation range in all comparisons except one, including both sexes. The MVDs between *P. kremani* and *P. apacheanus* ranged 8.3–11.7 % for males and 9.3–14.3 % for females, and the MVDs between *P. kremani* and *P. santarita* ranged 5.8–15.5 % for males and 10.9–16.2 % for females. The thinner metasoma of *P. kremani* is visually obvious by comparing the two views of the metasoma in Figs. 8 and 20 between it and *P. santarita*. See Appendix B for a complete presentation of the statistical data presented above.

Fixed finger morphometrics between sexes. Above we pointed out the large difference in the fixed finger morphometric comparisons between the sexes for *P. kremani* and *P. santarita*, the female *P. kremani* showing the largest MVDs. In Appendix B we present the results for all three species, where the metasomal segment length and width are compared to the fixed finger length between the sexes. For *P. apacheanus* and *P. santarita*, the MVDs are insignificant between their sexes, averaging 4.5–7.4 %. Whereas for *P. kremani*, we see an average MVD of 20.6 %, the female exhibiting relatively longer fingers than the male.

Acknowledgments

Special thanks goes to Melinda DeBoer-Ayrey for participating in 17 field trips to the Santa Rita Mountains, and Tom Miscione and Robert Troup for supplying important specimens. Thanks also goes to František Kovařík for providing photographs of key material, Victor Fet and Matthew Graham for making helpful suggestions to this paper, and to two anonymous reviewers.

References

AYREY, R. F. 2009. Sky island *Vaejovis*: A new species (Scorpiones: Vaejovidae). *Euscorpius*, 86: 1–12.

AYREY, R. F. 2012. A new *Vaejovis* from the Mogollon Highlands of Northern Arizona (Scorpiones: Vaejovidae). *Euscorpius*, 148: 1−13.

AYREY, R. F. 2013a. Reproduction in the "vorhiesi" group of the genus *Vaejovis* (Scorpiones: Vaejovidae). Part I. Clutch size. *Euscorpius*, 166: 1–15.

AYREY, R. F. 2013b. A new species of *Vaejovis* from the Mogollon Rim of northern Arizona (Scorpiones: Vaejovidae). *Euscorpius*, 176: 1−13.

AYREY, R. F. 2014. A new species of *Vaejovis* from chaparral habitat near Yarnell, Arizona (Scorpiones: Vaejovidae). *Euscorpius*, 188: 1−13.

AYREY, R. F. & M. E. SOLEGLAD. 2011. A new species of *Vaejovis* from Prescott, Arizona (Scorpiones: Vaejovidae). *Euscorpius*, 114: 1−15.

AYREY, R. F. & M. E. SOLEGLAD. 2014. New species of *Vaejovis* from the Santa Rita Mountains, southern Arizona (Scorpiones: Vaejovidae). *Euscorpius*, 183: 1−13.

AYREY, R. F. & M. M. WEBBER. 2013. A new *Vaejovis* C. L. Koch, 1836, the second known *vorhiesi* group species from the Santa Catalina Mountains of Arizona (Scorpiones: Vaejovidae). *ZooKeys,* 270: 21–35.

BRYSON, R. W., W. E. SAVARY & L. PRENDINI. 2013. Biogeography of scorpions in the *Pseudouroctonus minimus* complex (Vaejovidae) from south-western North America: implications of ecological specialization for pre-Quaternary diversification. *Journal of Biogeography*, 1–11.

CONTRERAS, G. A. & O. F. FRANCKE. 2014. Description of a new species of *Vaejovis* from Michoacán, Mexico (Arachnida: Scorpiones: Vaejovidae). *Revista Mexicana de Biodiversidad*, 85: 24–30.

CONTRERAS, G. A., O. F. FRANCKE & R. W. BRYSON. 2015. A new species of the "mexicanus" group of the genus *Vaejovis* C. L. Koch, 1836 from the Mexican state of Aguascalientes (Scorpiones: Vaejovidae). *Zootaxa*, 3936 (1): 131–140.

FRANCKE, O. F. 2009. Description of a new species of troglophile *Pseudouroctonus* (Scorpiones: Vaejovidae) from Coahuila, Mexico. *Texas Memorial Museum Speleological Monographs, 7. Studies on the Cave and Endogean Fauna of North America*, V: 11–18.

FRANCKE, O. F. & W. E. SAVARY. 2006. A new troglobitic *Pseudouroctonus* Stahnke (Scorpiones: Vaejovidae) from northern México. *Zootaxa*, 1302: 21–30.

GERTSCH, W. J. & M. E. SOLEGLAD. 1972. Studies of North American scorpions of the genera *Uroctonus* and *Vejovis*. *Bulletin of the American Museum of Natural History*, 148(4): 549–608.

GONZÁLEZ SANTILLÁN, E., W. D. SISSOM & T. M. PÉREZ. 2004. Description of the male *Vaejovis sprousei* Sissom, 1990 (Scorpiones: Vaejovidae). Pp. 9–12 *in*: Cokendolpher, J. C. & J. R. Reddell (eds.). *Studies on the Cave and Endogean Fauna of North America IV*, *Texas Memorial Museum Speleological Monographs* 6.

HJELLE, J. T. 1974. Observations on the birth and post-birth behavior of *Syntropis macrura* Kraepelin (Scorpiones: Vaejovidae). *Journal of Arachnology*, 1: 221–227.

JARVIS, L. R., W. D. SISSOM & R. N. HENSON. 2004. Description of the male of *Vaejovis chisos* Sissom (Scorpiones, Vaejovidae) from Texas, U.S.A., with comments on morphometric and meristic variation in the species. *Entomological News*, 115 (4): 207–211.

KOVAŘÍK, F. & A. A. OJANGUREN AFFILASTRO. 2013. Illustrated catalog of scorpions Part II. Bothriuridae; Chaerilidae; Buthidae I., genera *Compsobuthus*, *Hottentotta*, *Isometrus*, *Lychas*, and *Sassanidotus*. Prague: Clairon Production, 400 pp.

MATTONI C. I. 2007. The genus *Bothriurus* (Scorpiones, Bothriuridae) in Patagonia. *Insect Systematics & Evolution*, 38(1): 1–22.

McWEST, K. J. 2009. Tarsal spinules and setae of vaejovid scorpions (Scorpiones: Vaejovidae). *Zootaxa*, 1–126.

OJANGUREN AFFILASTRO A. A., P. AGUSTO, J. PIZARRO-ARAYA & C. I. MATTONI. 2007. Two new scorpion species of genus *Brachistosternus* (Scorpiones: Bothriuridae) from northern Chile. *Zootaxa*, 1623: 55–68.

OJANGUREN AFFILASTRO A. A., F. F. CAMPÓN, S. L. SILNIK & C. I. MATTONI. 2009. The genus *Orobothriurus* Maury in central Argentina with description of a new species from El Nevado mountain chain in Mendoza Province (Scorpiones: Bothriuridae). *Zootaxa*, 2209: 28–42.

SISSOM, W. D. 1989. Systematic studies on *Vaejovis granulatus* Pocock and *Vaejovis pusillus* Pocock with descriptions of six new related species (Scorpiones, Vaejovidae). *Revue Arachnologique*, 8(9): 131–157.

SISSOM, W. D. & E. GONZÁLEZ SANTILLÁN. 2004. A new species and new records for the *Vaejovis nitidulus* group, with a key to the Mexican species (Scorpiones: Vaejovidae). Pp. 1–8 in: Cokendolpher, J. C. & J. R. Reddell (eds.). *Studies on the Cave and Endogean Fauna of North America IV, Texas Memorial Museum Speleological Monographs* 6: 1–8.

SOLEGLAD, M. E. 1973. Scorpions of the mexicanus group of the genus *Vejovis* (Scorpionida, Vejovidae). *The Wasmann Journal of Biology*, 31(2): 351–372.

SOLEGLAD, M. E. & V. FET. 2003a. The scorpion sternum: structure and phylogeny (Scorpiones: Orthosterni). *Euscorpius*, 5: 1–34.

SOLEGLAD, M. E. & V. FET. 2003b. High-level systematics and phylogeny of the extant scorpions (Scorpiones: Orthosterni). *Euscorpius*, 11: 1–175.

SOLEGLAD, M. E. & V. FET. 2006. Contributions to scorpion systematics. II. Stahnkeini, a new tribe in scorpion family Vaejovidae (Scorpiones: Chactoidea). Euscorpius, 40: 1–32.

SOLEGLAD, M. E. & V. FET. 2008. Contributions to scorpion systematics. III. subfamilies Smeringurinae and Syntropinae (Scorpiones: Vaejovidae). *Euscorpius*, 71: 1–115.

SOLEGLAD, M. E. & W. D. SISSOM. 2001. Phylogeny of the family Euscorpiidae Laurie, 1896: a major revision. Pp. 25–111 *in* Fet, V. & P. A. Selden (eds.). *Scorpions 2001. In memoriam Gary A. Polis*. Burnham Beeches, Bucks: British Arachnological Society.

STAHNKE, H. L. 1971. Scorpion nomenclature and mensuration. *Entomological News,* 81: 297–316.

STAHNKE, H. L. 1974. Revision and keys to the higher categories of Vejovidae. *Journal of Arachnology*, 1(2): 107–141.

STOCKWELL, S. A. 1992. Systematic observations on North American Scorpionida with a key and checklist of the families and genera. *Journal of Medical Entomology*, 29(3): 407–422.

TATE, A. E., R. R. RIDDLE, M. E. SOLEGLAD & M. R. GRAHAM. 2013. *Pseudouroctonus peccatum*, a new scorpion from the Spring Mountains near Las Vegas, Nevada (Scorpiones: Vaejovidae). *ZooKeys*, 364: 29–45.

VACHON, M. 1974. Étude des caractères utilisés pour classer les familles et les genres de Scorpions (Arachnides). 1. La trichobothriotaxie en Arachnologie, Sigles trichobothriaux et types de trichobothriotaxie chez les Scorpions. *Bulletin du Muséum National d'Histoire Naturelle, Paris,* (3), 140 (Zool. 104), mai–juin 1973: 857–958.

Appendix A
Trichobothrial Patterns of Select Species of *Pseudouroctonus* and *Uroctonites*

In this Appendix we show trichobothrial patterns of species of interest in the genus *Pseudouroctonus* and *Uroctonites*, most of which, are illustrated for the first time. The choice of species is based, in part, on the molecular-based study of Bryson et al. (2013: figs. 3–4) which formed their "*P. minimus* complex" as well as others discussed in this paper. In the body of this paper these patterns are discussed in context with the patterns of the two new species described in this paper, *P. santarita* and *P. kremani*, and the species P. *apacheanus*.

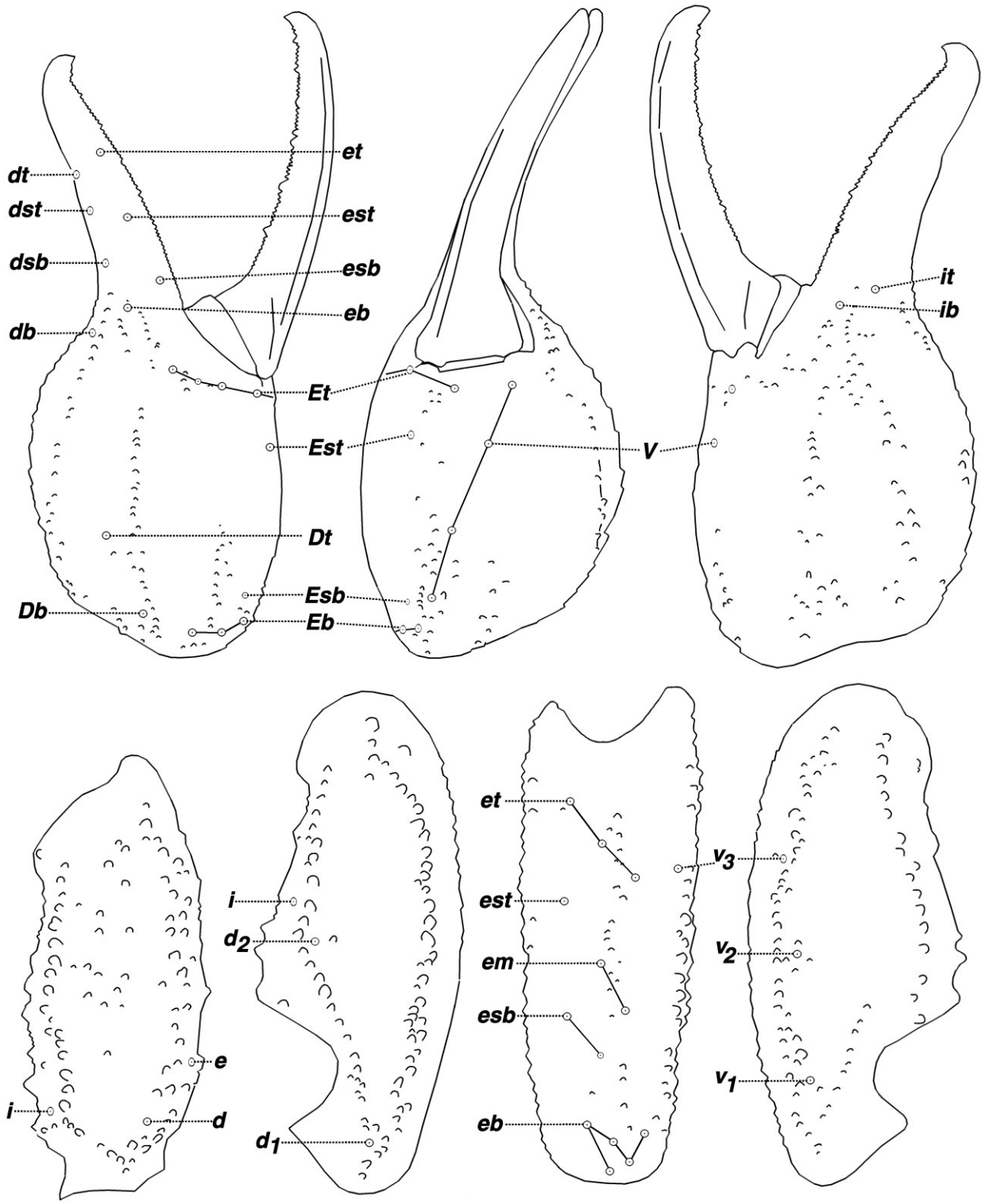

Figure A-1: *Pseudouroctonus minimus thompsoni*, male, Santa Cruz Island, Santa Barbara Co., California, USA. Trichobothrial pattern.

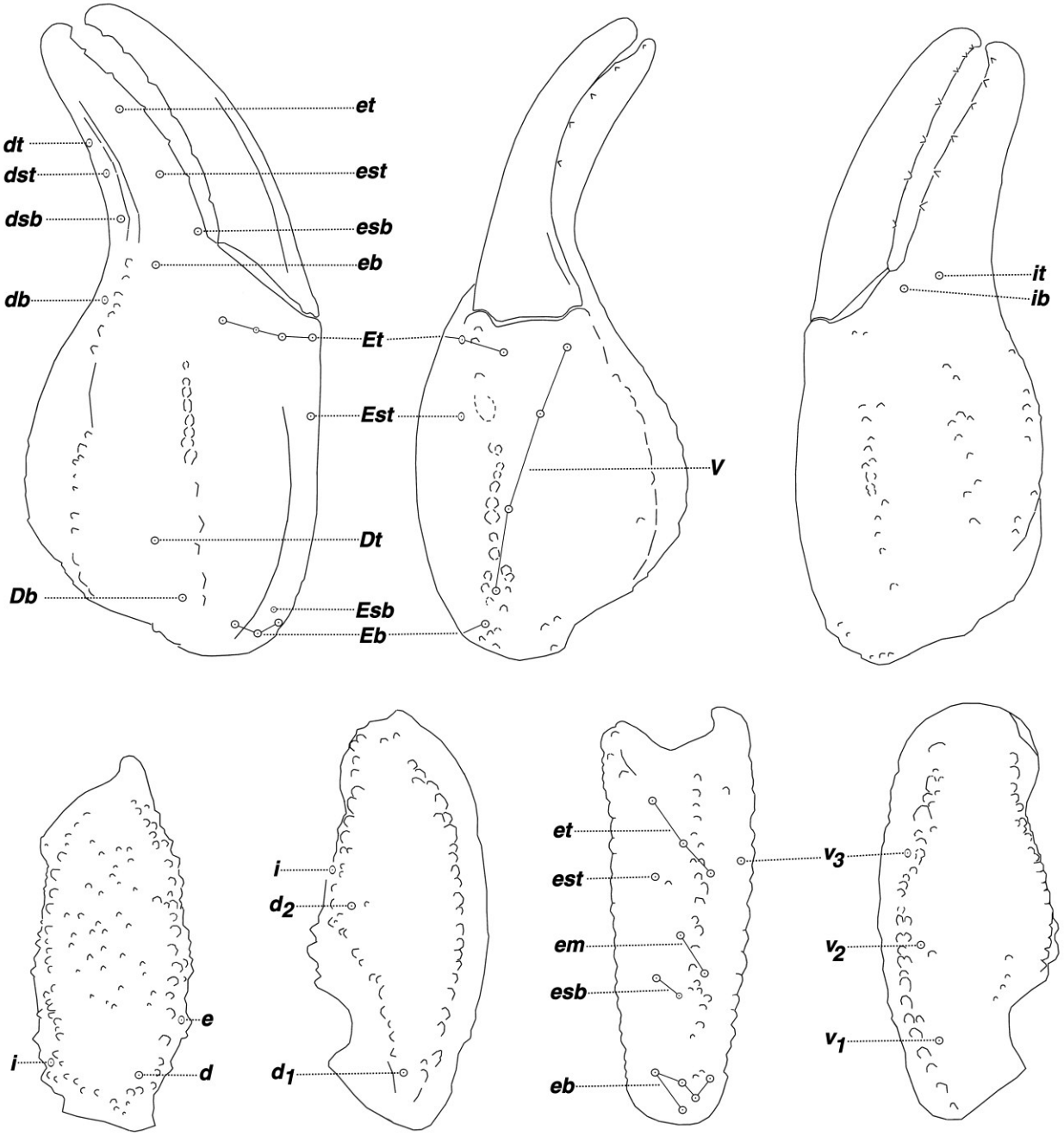

Figure A-2: *Pseudouroctonus minimus castaneus*, male, Vista, San Diego Co., California, USA. Trichobothrial pattern.

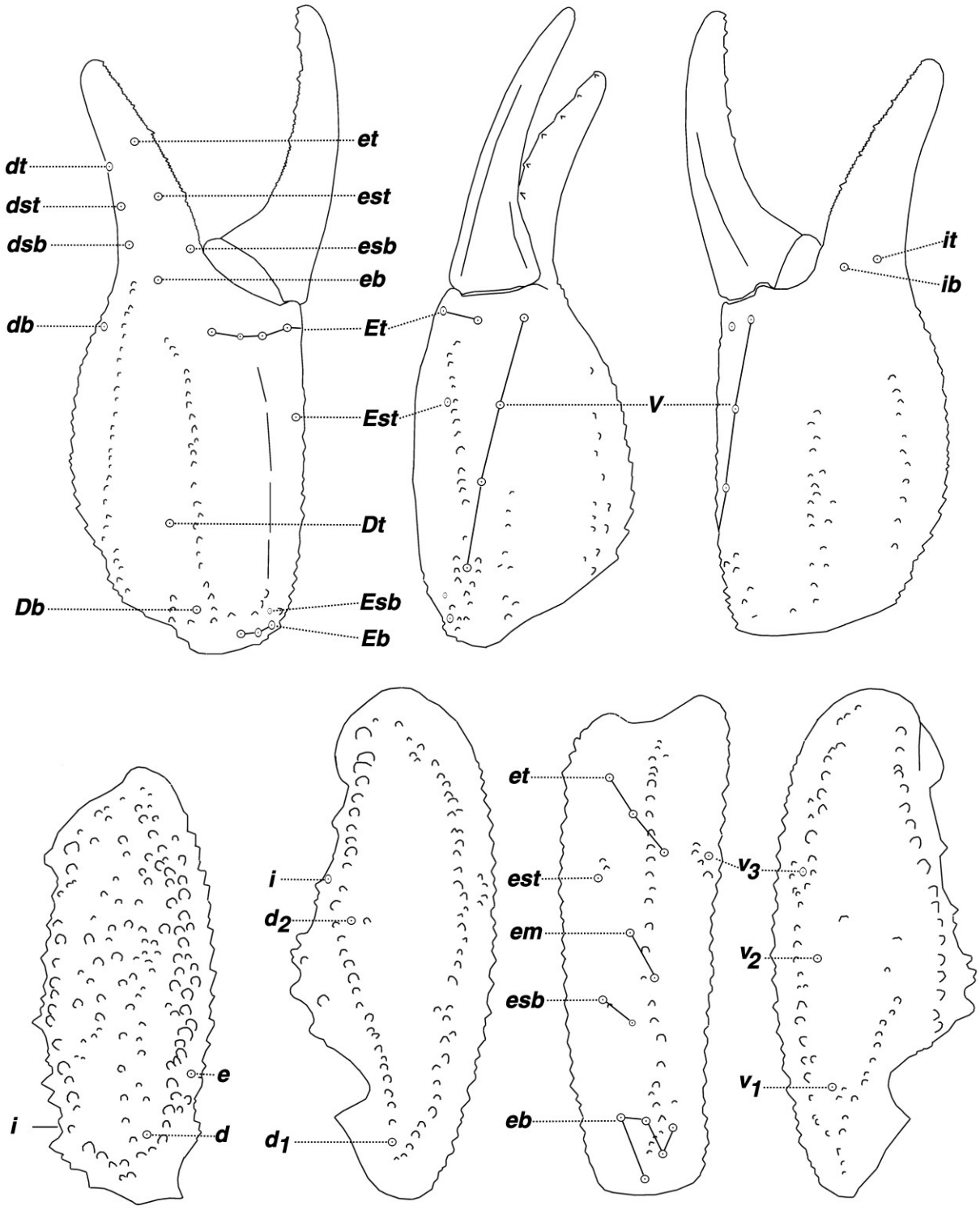

Figure A-3: *Pseudouroctonus andreas*, male, Chariot Canyon, ABDSP, San Diego Co., California, USA. Trichobothrial pattern.

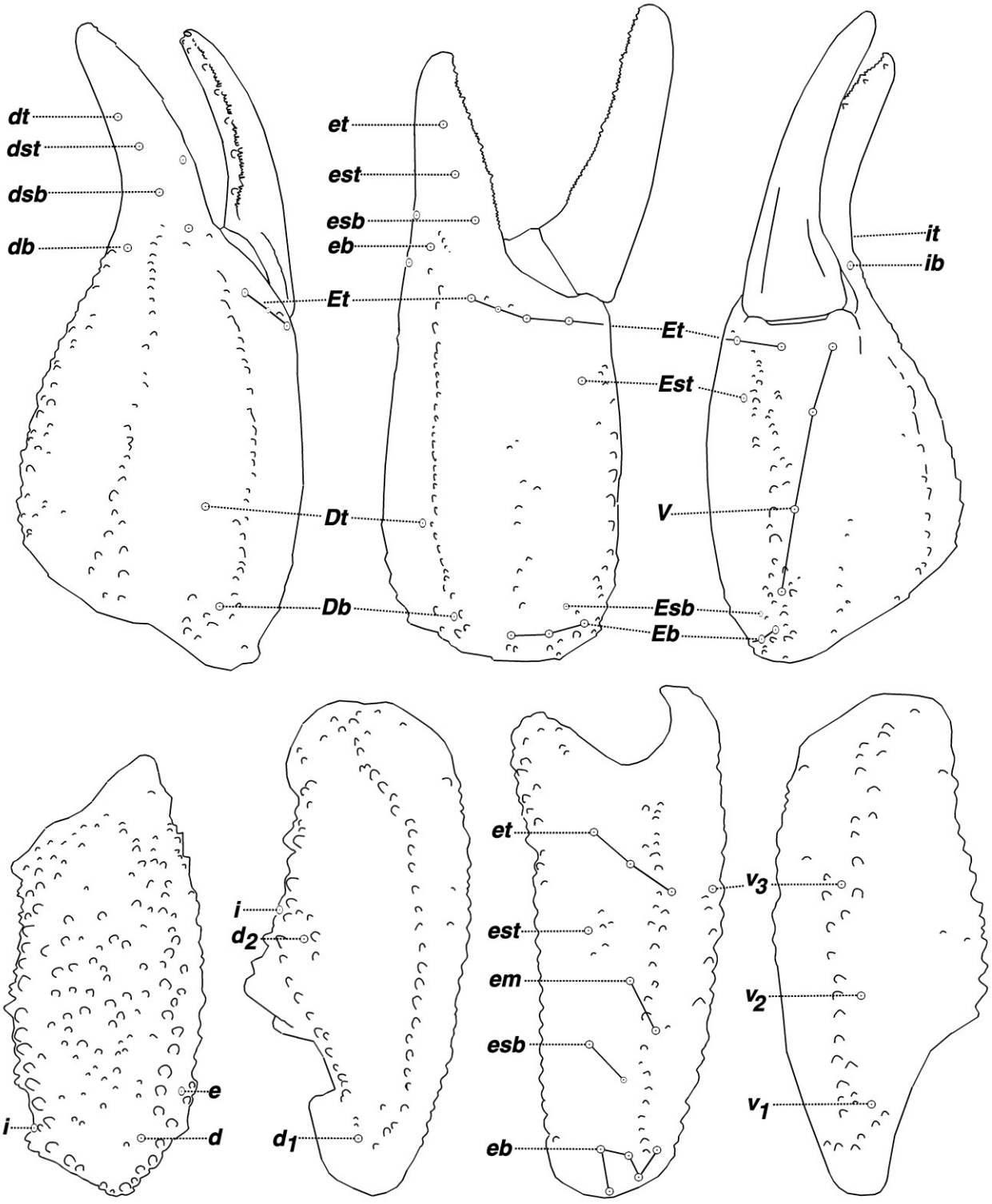

Figure A-4: *Pseudouroctonus chicano*, male, 20 km E. Guachochi, Chihuahua, Mexico. Trichobothrial pattern. Illustration is based on a photograph courtesy of František Kovařík.

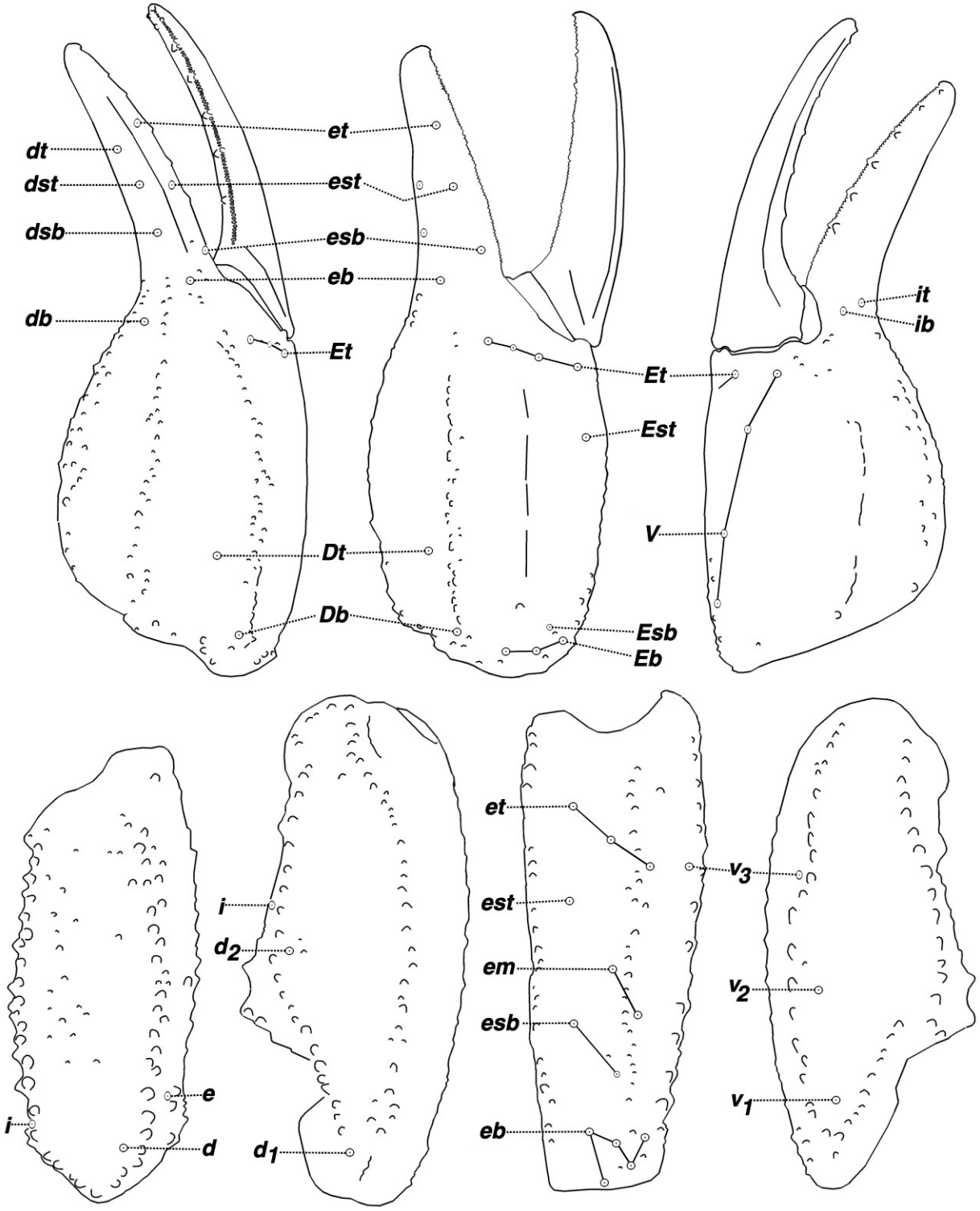

Figure A-5: *Pseudouroctonus rufulus*, female holotype, Punta Banda, Baja California Norte, Mexico. Trichobothrial pattern. Illustration is based on a photograph courtesy of František Kovařík.

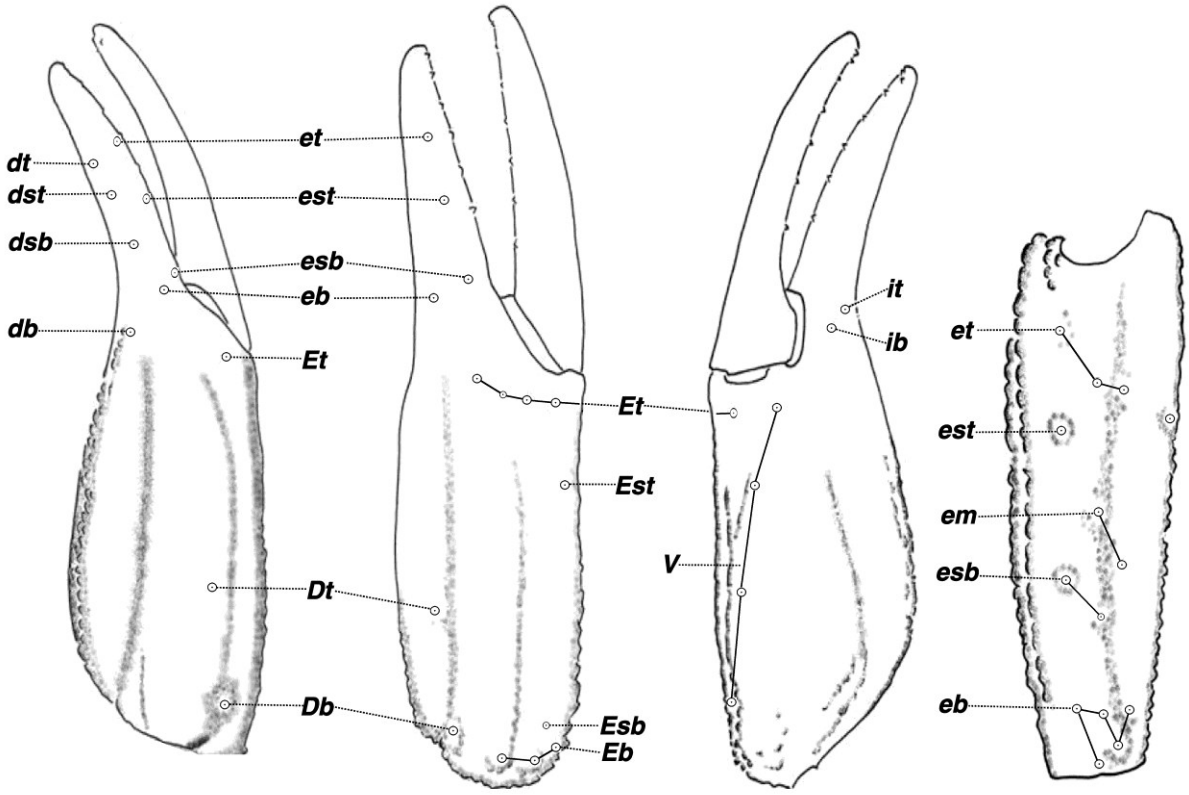

Figure A-6: *Pseudouroctonus savvasi*, male holotype, Cueva de la Casa Blanca, Coahuila, Mexico. Partial trichobothrial pattern after Francke, 2009, figs. 6–9, in part.

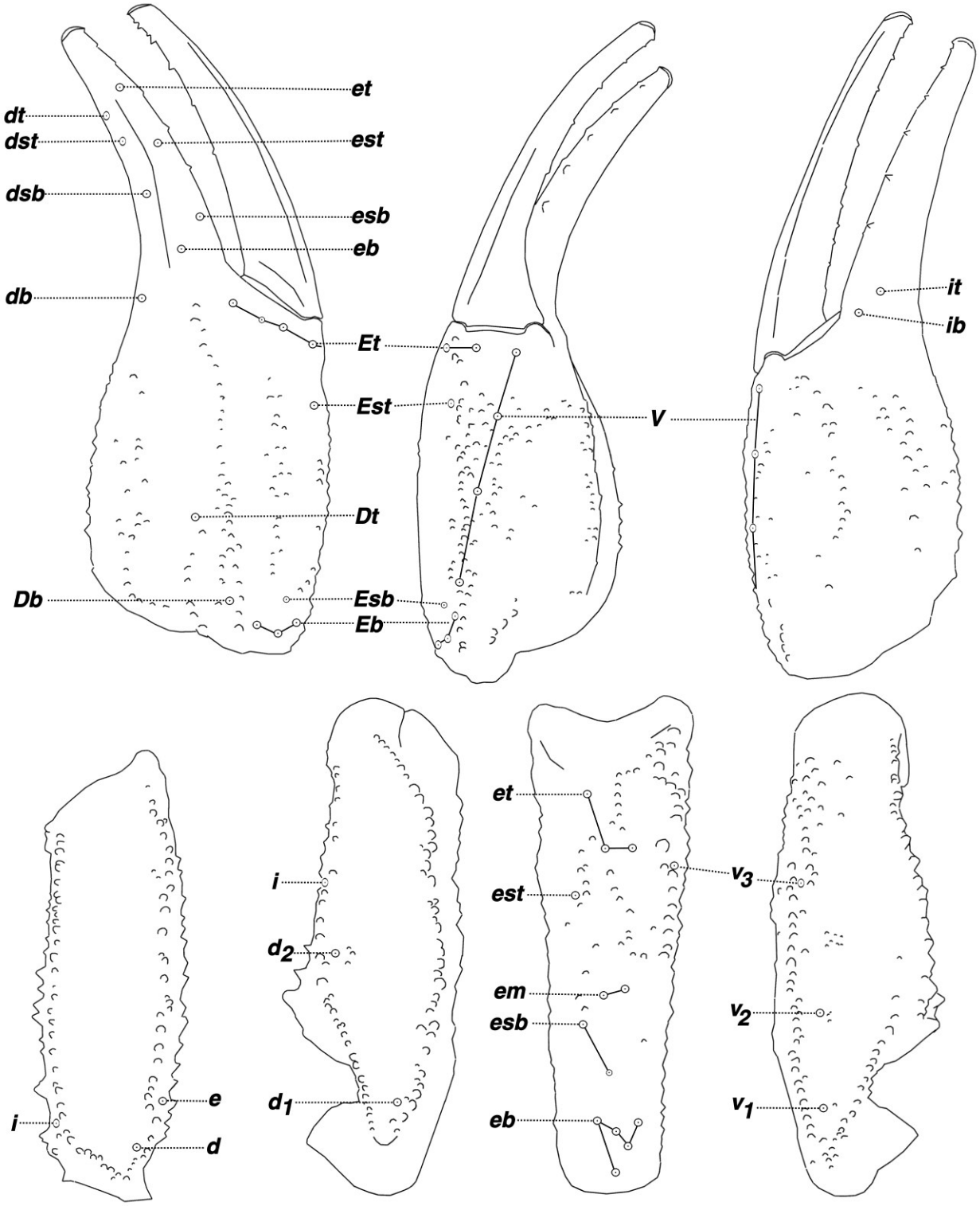

Figure A-7: *Pseudouroctonus reddelli*, male, Gem Cave, Comal Co., Texas, USA. Trichobothrial pattern.

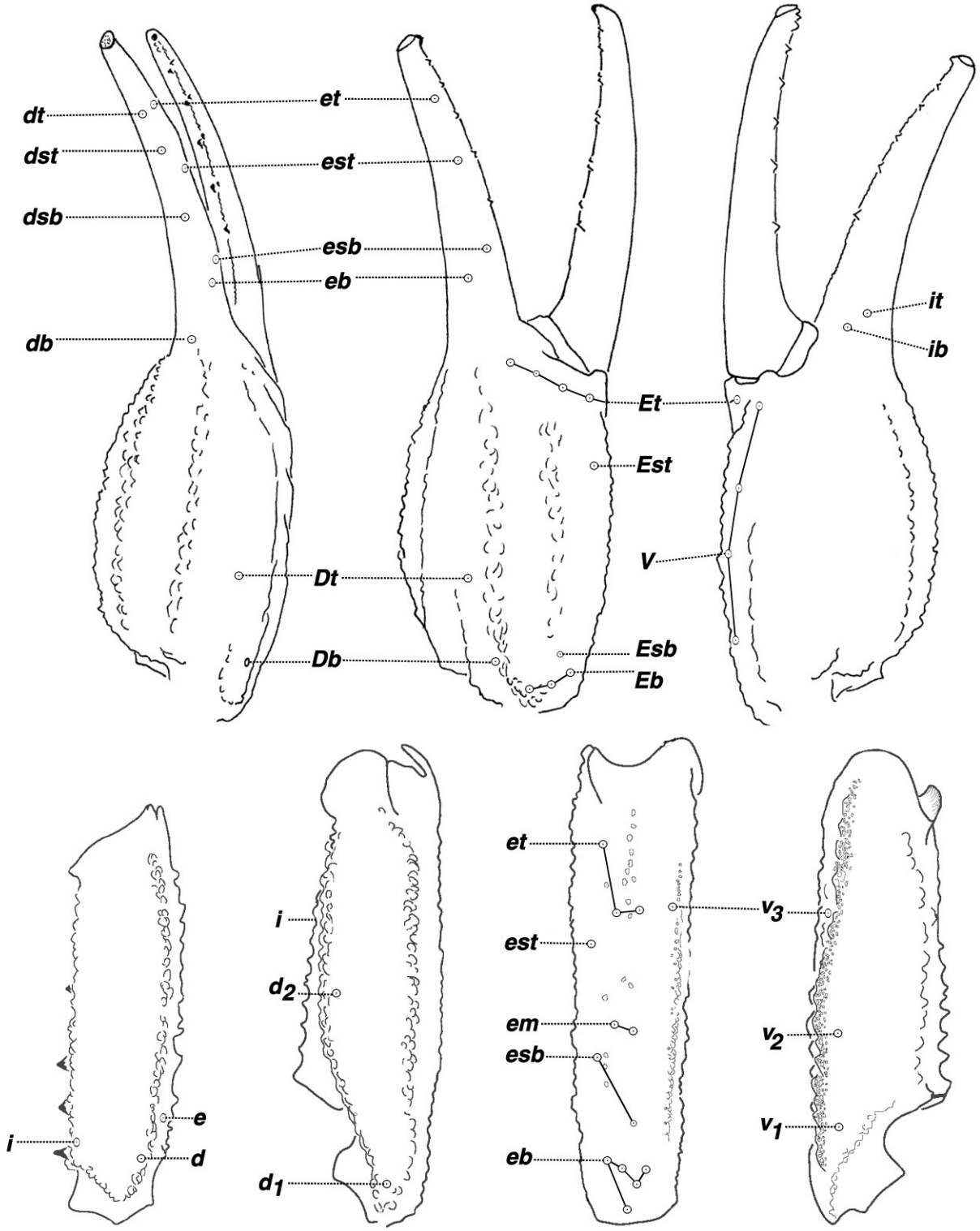

Figure A-8: *Pseudouroctonus sprousei*, male holotype, El Abra Cave, El Remolino, Coahuila, Mexico. Trichobothrial pattern (after Francke & Savary, 2006, figs. 5–11, in part).

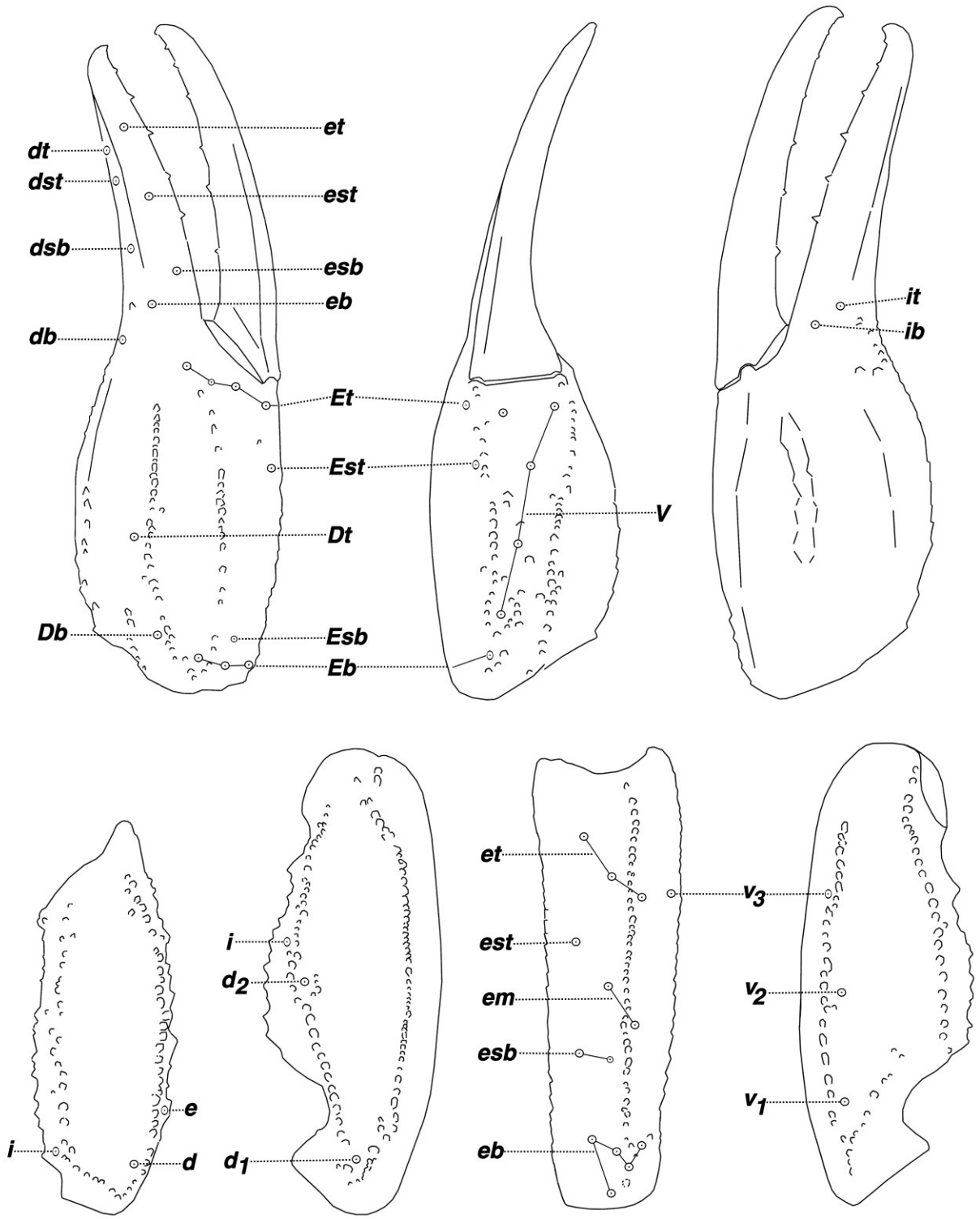

Figure A-9: *Pseudouroctonus iviei*, female, Little French Creek, Trinity Co., California, USA. Trichobothrial pattern.

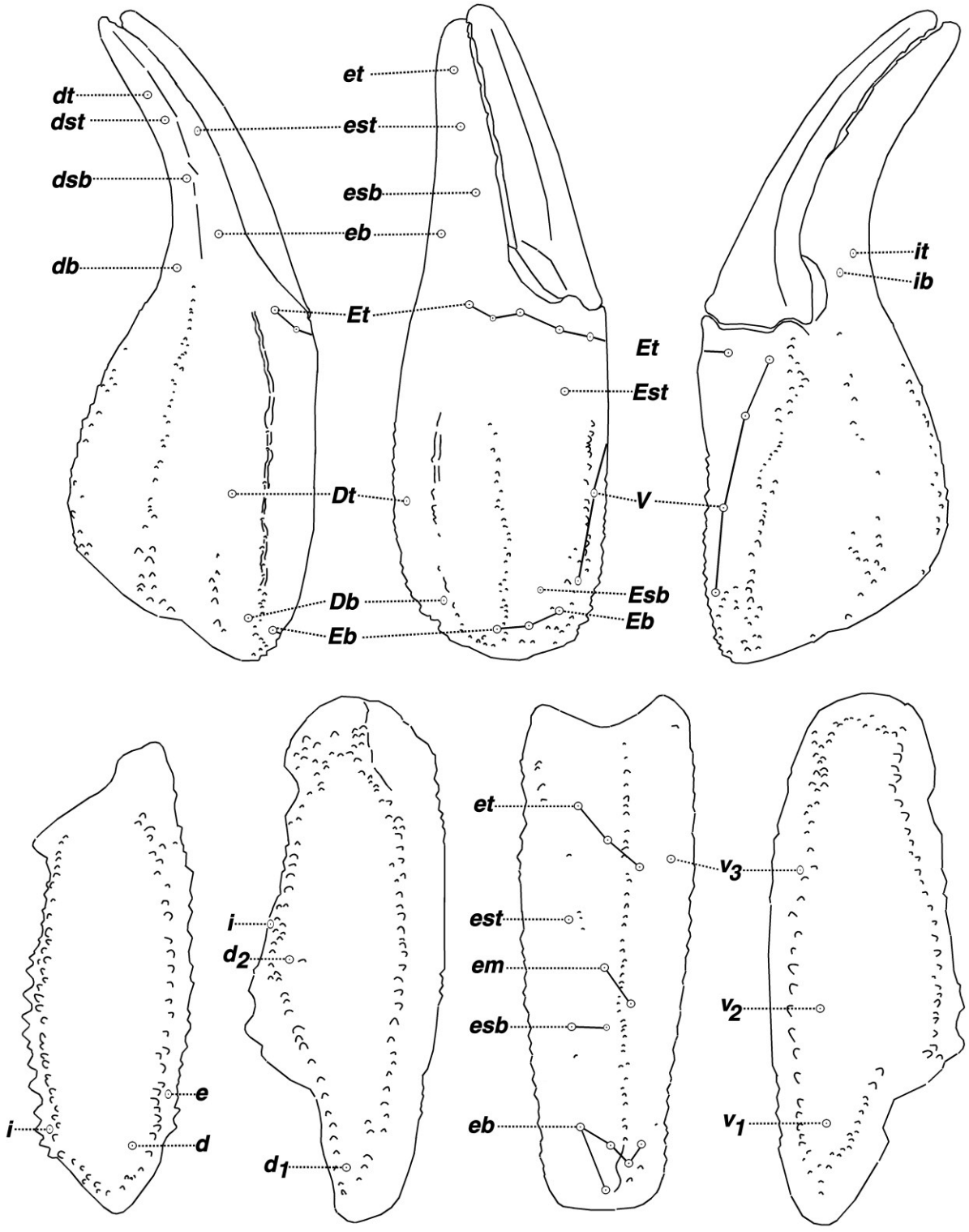

Figure A-10: *Pseudouroctonus glimmei*, female, Cache Creek Regional Park, Lake Co., California, USA. Trichobothrial pattern. Illustration is based on a photograph courtesy of František Kovařík.

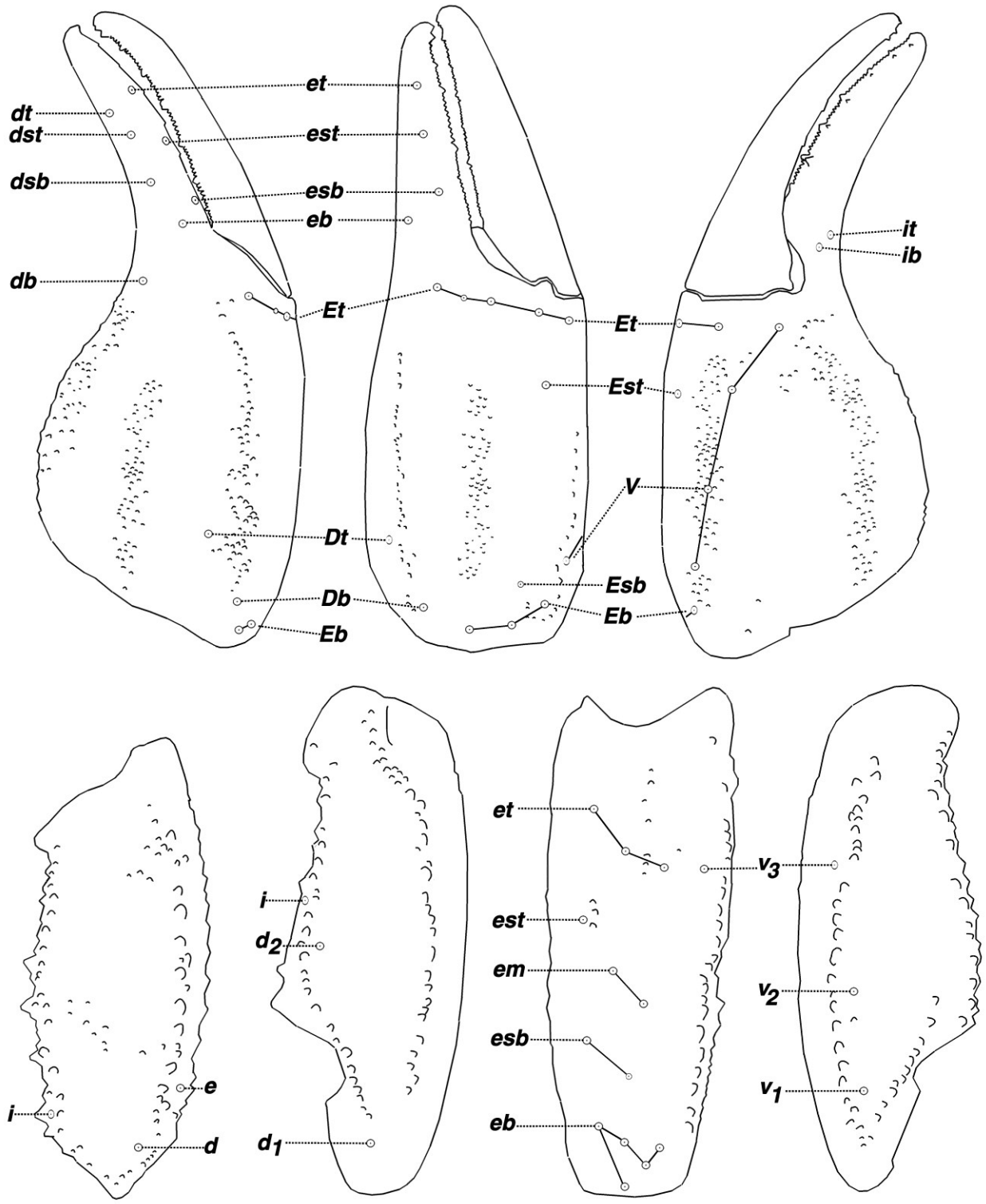

Figure A-11: *Pseudouroctonus lindsayi*, male, Sierra Laguna, Baja California, Mexico. Trichobothrial pattern. Illustration is based on a photograph courtesy of František Kovařík.

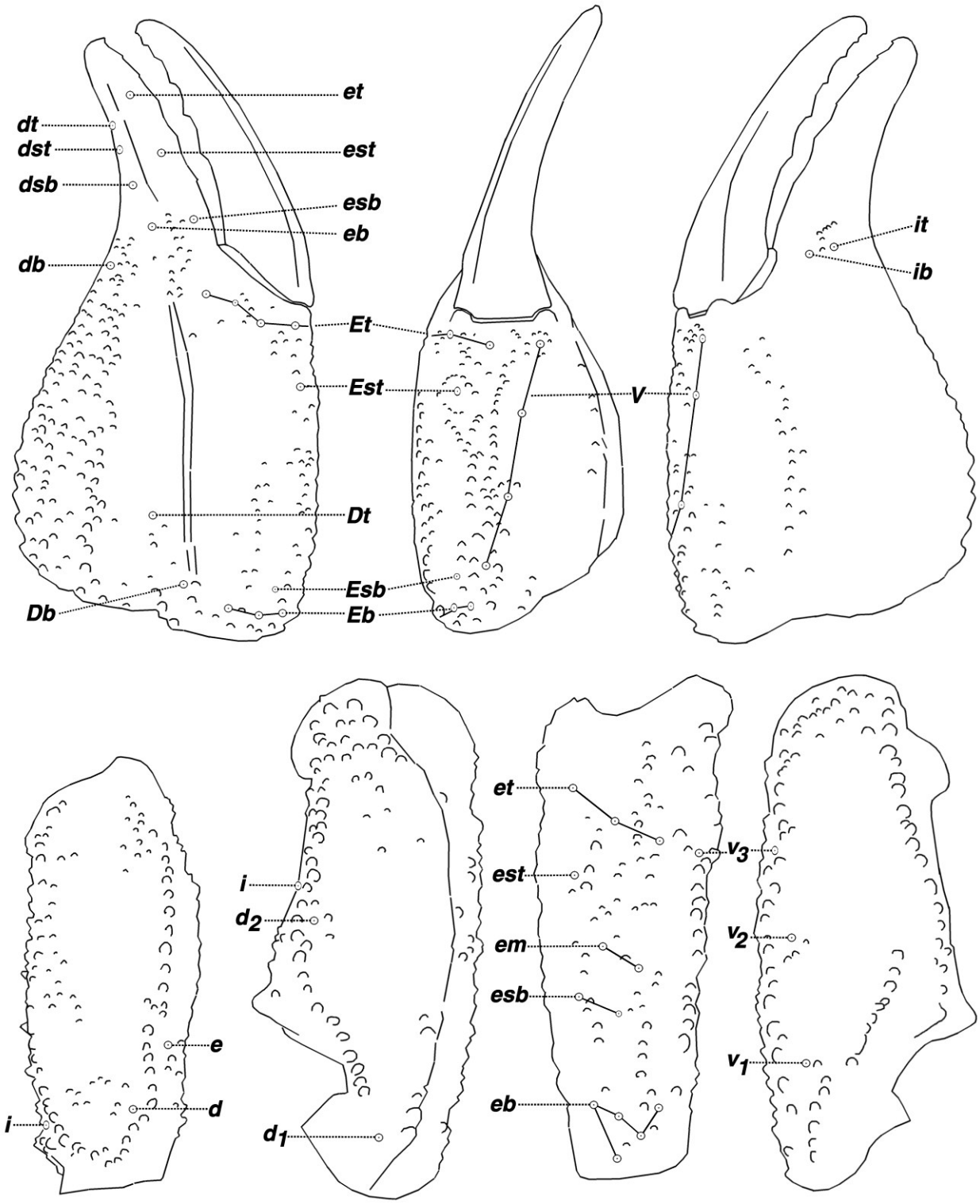

Figure A-12: *Uroctonites huachuca*, male, Huachuca Mountains, Cochise Co., Arizona, USA. Trichobothrial pattern.

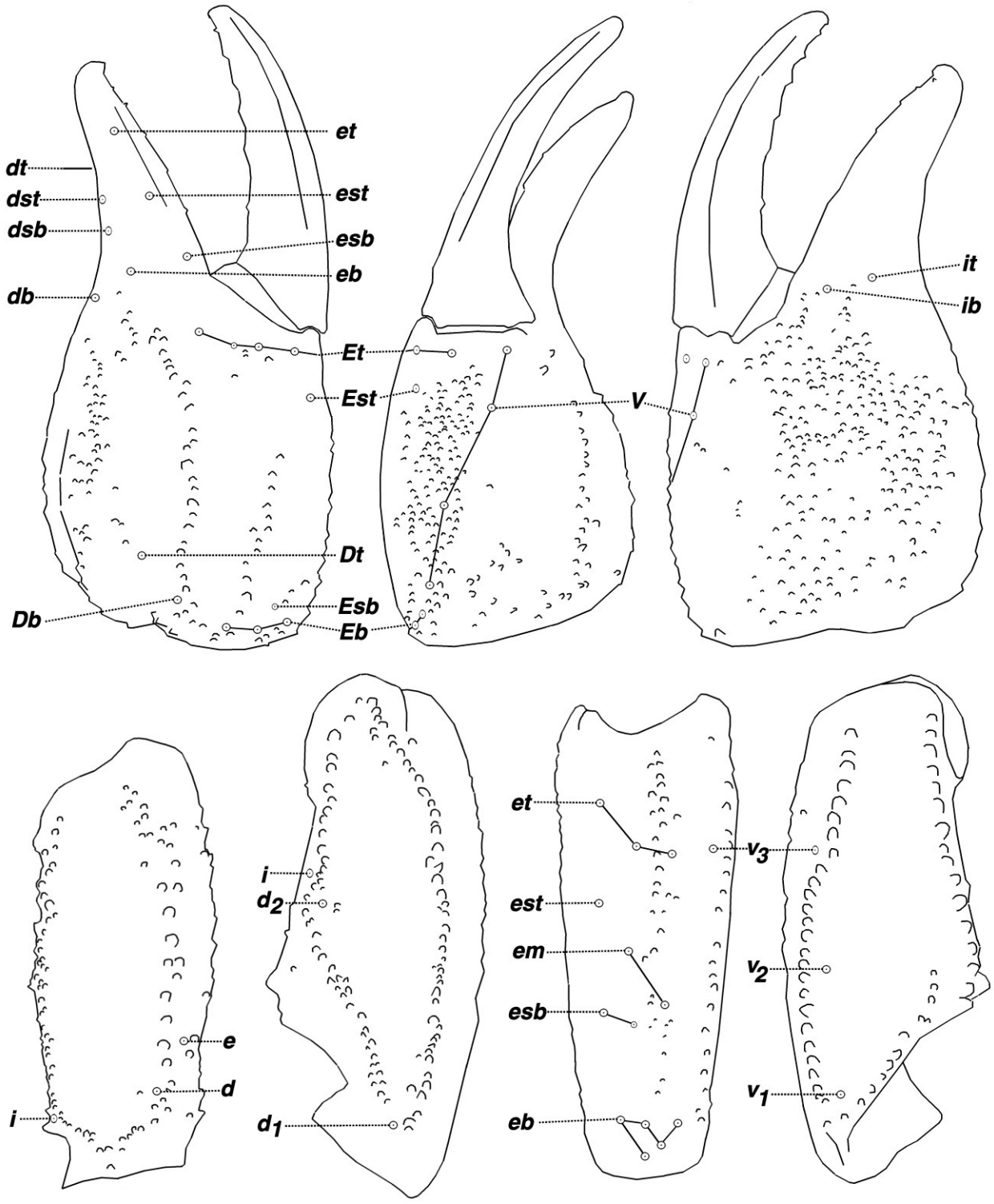

Figure A-13: *Uroctonites montereus*, male, Hastings Natural History Reservation, Monterey Co., California, USA. Trichobothrial pattern.

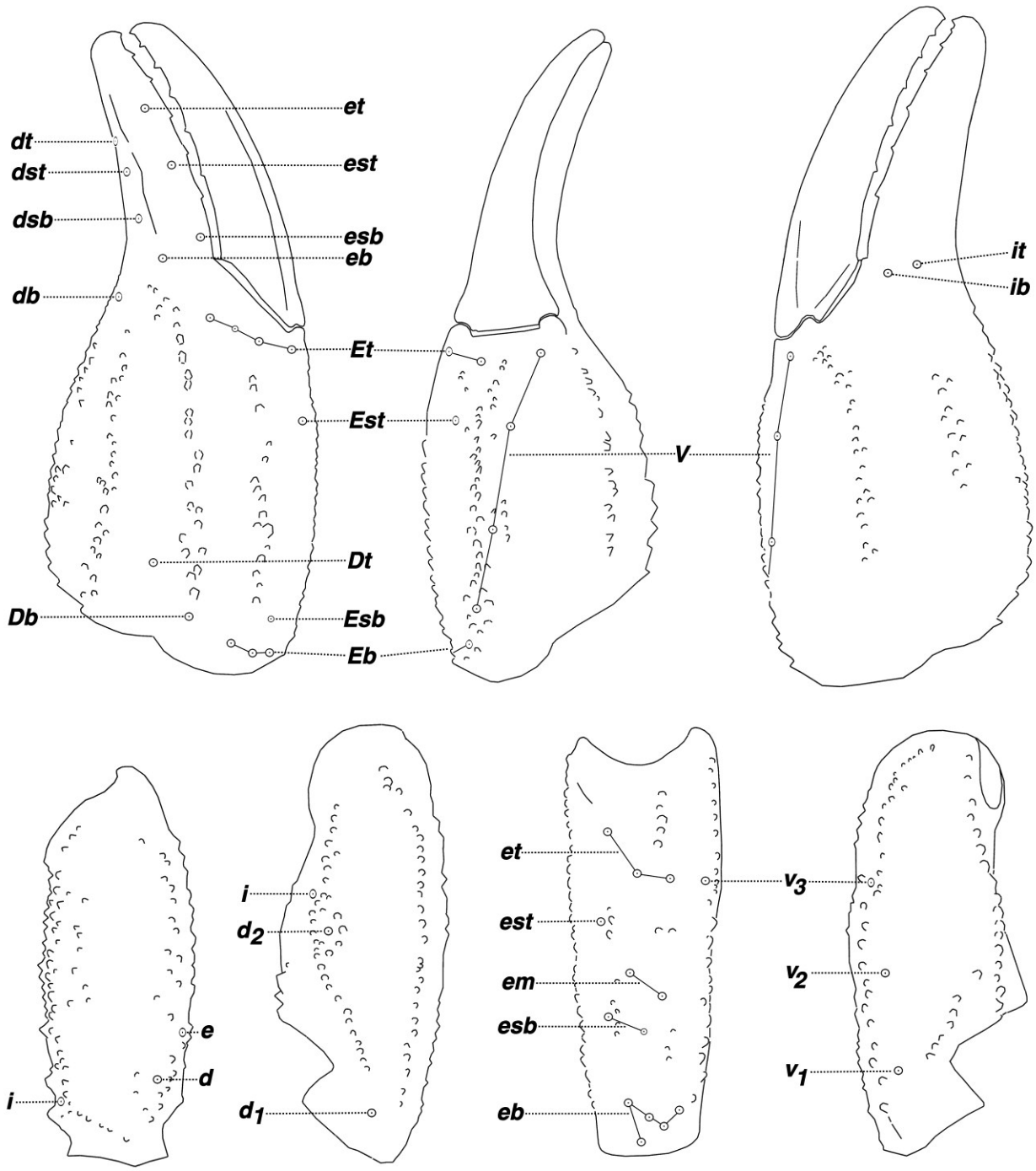

Figure A-14: *Uroctonites giulianii*, female, Lead Canyon, Inyo Co., California, USA. Trichobothrial pattern.

Appendix B
Statistical Results from Morphometric and Meristic Analysis

This appendix presents all statistical data used in this paper for the establishment of diagnostic characters. The data is based on the analysis of eighteen specimens, six *Pseudouroctonus apacheanus*, five *P. kremani*, and seven *P. santarita*. All specimens studied were adult except for one juvenile female specimen of *P. kremani* which was studied only for median denticle (*MD)* counts of the chelal fixed finger (i.e., morphometrics were *not* calculated due to its juvenile status). Showing statistical support for the morphological, morphometric and meristic based diagnostic characters established in this paper, this appendix provides detailed data for the following:

a. statistical data of the overall structure of the mating plug and the present/absence of a distal crest on the lamina terminus are provided for all examined male specimens.

b. the relative slenderness of the metasoma in species *P. kremani* is demonstrated by comparing each segment's length to its width. A histogram (Figure B-1) of all five segments for both sexes is shown and MVD comparisons are provided across all three species and genders.

c. the relative length of the chelal fingers is analysed by comparing each metasomal segment's length and width to the length of both fingers, fixed and movable. It is shown that species *P. santarita* has the overall shortest chelal fingers. A histogram (Figure B-2) of all five segment widths compared to the fixed finger length is shown for both sexes and MVD comparisons are provided.

d. the fixed finger's relative length is further analyzed by providing the number of median denticles (*MD*) found in each row (i.e., six *MD* rows occur on this finger for all three species) further supporting the observations that *P. santarita* has the shortest fixed finger for the three species, since it also has the fewest number of *MD* denticles.

e. unlike the other two species, *P. kremani*'s *MD* denticle counts are noticeably larger in the female than the male. We show that this statistic is caused by the relatively longer fixed fingers found in the female as compared to the other two species, where the length differences between sexes are minmal.

f. pectinal tooth count data is presented.

Data in this appendix is presented is as follows: minimum–maximum (mean) (±standard deviation) [number of samples] {mean: plus–minus standard deviation} (coefficient of variability). MP = mating plug, MVD = mean value difference (%). L = length, W = width, I, I–L, I–W = metasomal segment I, length, width, II, II–L, II–W = metasomal segment II, length, width, III, III–L, III–W = metasomal segment III, length, width, IV, IV–L, IV–W = metasomal segment IV, IV–L, IV–W, V, V–L, V–W = metasomal segment V, length, width, FL = fixed finger length, and ML = movable finger length.

Hemispermatophore and Mating Plug Data
(identified by specimen ID, left/right hemispermatophore)

***P. santarita*: (3 males)**	**RA953**	**RA1104**	**RA1102**	**Total**
Brace-A projection	Yes/Yes	Yes/-	-/-	3
Brace-B projection	Yes/Yes	Yes/-	-/-	3
Lamina crest present	Yes/Yes	Yes/Yes	Yes/Yes	6
***P. kremani*: (2 males)**	**RA707**	**RA1110**		**Total**
Brace-A projection	No/No	-/-		2
Brace-B projection	No/No	-/-		2
Lamina crest present	No/No	No/No		4
***P. apacheanus*: (3 males)**	**RA836**	**RA1097**	**RA2133**	**Total**
Brace-A projection	No/No	-/-	-/No	3
Brace-B projection	No/No	-/-	-/No	3
Lamina crest present	Yes/Yes	-/-	Yes/Yes	4

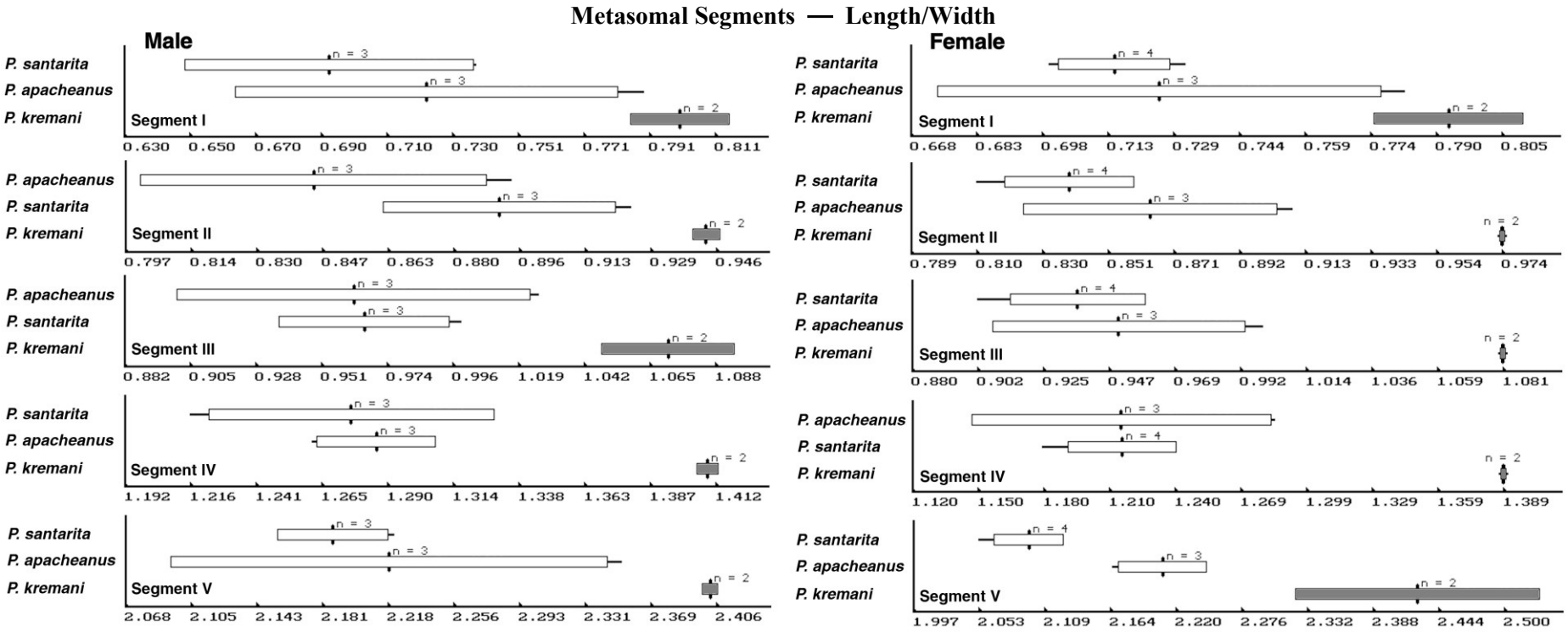

Figure B-1: Histograms above demonstrate that *P. kremani* (dark bars) has the thinnest metasoma when the metasomal segment's length is compared to its width.

	P. apacheanus	***P. kremani***	***P. santarita***
I:			
♂:	0.681–0.789 (0.723) (±0.058) [3] {0.664–0.781} (0.081)	0.789–0.811 (0.800) (±0.015) [2] {0.785–0.815] (0.019)	0.650–0.738 (0.693) (±0.044) [3] {0.649–0.737} (0.064)
♀:	0.683–0.783 (0.726) (±0.051) [3] {0.674–0.777} (0.071)	0.780–0.805 (0.793) (±0.017) [2] {0.775–0.810} (0.022)	0.700–0.732 (0.715) (±0.013) [4] {0.702–0.728} (0.018)
II:			
♂:	0.814–0.895 (0.845) (±0.044) [3] {0.801–0.888} (0.052)	0.941–0.946 (0.944) (±0.003) [2] {0.940–0.947} (0.004)	0.872–0.925 (0.892) (±0.029) [3] {0.863–0.921} (0.033)
♀:	0.833–0.909 (0.864) (±0.040) [3] {0.824–0.904} (0.046)	0.974–0.974 (0.974) (±0.000) [2] {0.974–0.974} (0.000)	0.810–0.854 (0.839) (±0.020) [4] {0.819–0.859} (0.024)
III:			
♂:	0.905–1.027 (0.962) (±0.061) [3] {0.901–1.024} (0.064)	1.056–1.088 (1.072) (±0.023) [2] {1.049–1.095} (0.022)	0.947–1.000 (0.966) (±0.030) [3] {0.936–0.995} (0.031)
♀:	0.925–1.000 (0.951) (±0.043) [3] {0.908–0.993} (0.045)	1.081–1.081 (1.081) (±0.000) [2] {1.081–1.081} (0.000)	0.902–0.950 (0.937) (±0.023) [4] {0.914–0.960] (0.025)
IV:			
♂:	1.262–1.306 (1.286) (±0.022) [3] {1.264–1.308} (0.017)	1.406–1.412 (1.409) (±0.004) [2] {1.405–1.413} (0.003)	1.216–1.316 (1.276) (±0.053) [3] {1.223–1.329} (0.041)
♀:	1.150–1.286 (1.215) (±0.068) [3] {1.147–1.283} (0.056)	1.389–1.389 (1.389) (±0.000) [2] {1.389–1.389} (0.000)	1.179–1.231 (1.216) (±0.025) [4] {1.191–1.240} (0.020)
V:			
♂:	2.105–2.353 (2.219) (±0.125) [3] {2.094–2.344} (0.056)	2.400–2.406 (2.403) (±0.004) [2] {2.399–2.408} (0.002)	2.162–2.222 (2.187) (±0.031) [3] {2.156–2.218} (0.014)
♀:	2.167–2.237 (2.210) (±0.038) [3] {2.172–2.247} (0.017)	2.353–2.500 (2.426) (±0.104) [2] {2.322–2.530} (0.043)	2.053–2.118 (2.096) (±0.029) [4] {2.067–2.125} (0.014)

The above data shows that species *P. kremani* has the thinnest metasoma, as exhibited for all five segments. See MVD comparisons below.

Chelal Finger Morphometrics Compared to Metasomal Segment Lengths and Widths

		P. apacheanus	*P. kremani*	*P. santarita*
Segment I				
L/FL	♂	0.588–0.604 (0.597) (±0.008) [3] {0.589–0.605} (0.014)	0.667–0.682 (0.674) (±0.011) [2] {0.664–0.685} (0.016)	0.650–0.721 (0.677) (±0.030) [3] {0.638–0.715} (0.057)
	♀	0.549–0.621 (0.587) (±0.036) [3] {0.551–0.624} (0.061)	0.533–0.579 (0.556) (±0.032) [2] {0.524–0.588} (0.058)	0.638–0.667 (0.652) (±0.012) [4] {0.641–0.664} (0.018)
W/FL	♂	0.745–0.887 (0.831) (±0.075) [3] {0.755–0.906} (0.091)	0.822–0.864 (0.843) (±0.029) [2] {0.814–0.872} (0.035)	0.955–1.000 (0.977) (±0.023) [3] {0.954–0.100} (0.023)
	♀	0.793–0.833 (0.810) (±0.021) [3] {0.789–0.831} (0.026)	0.683–0.719 (0.701) (±0.025) [2] {0.676–0.727} (0.036)	0.872–0.952 (0.913) (±0.033) [4] {0.880–0.946} (0.036)
L/ML	♂	0.429–0.448 (0.440) (±0.010) [3] {0.430–0.451} (0.024)	0.469–0.484 (0.476) (±0.011) [2] {0.466–0.487} (0.022)	0.456–0.500 (0.475) (±0.023) [3] {0.452–0.497} (0.048)
	♀	0.406–0.450 (0.429) (±0.022) [3] {0.407–0.452} (0.052)	0.395–0.413 (0.404) (±0.012) [2] {0.391–0.416} (0.031)	0.441–0.476 (0.459) (±0.014) [4] {0.445–0.474} (0.031)
W/ML	♂	0.567–0.653 (0.611) (±0.043) [3] {0.569–0.654} (0.070)	0.594–0.597 (0.595) (±0.002) [2] {0.593–0.597} (0.004)	0.677–0.702 (0.686) (±0.014) [3] {0.671–0.700} (0.020)
	♀	0.575–0.608 (0.592) (±0.017) [3] {0.576–0.609} (0.028)	0.506–0.513 (0.509) (±0.004) [2] {0.505–0.514} (0.000)	0.603–0.667 (0.643) (±0.028) [4] {0.615–0.671} (0.043)
Segment II				
L/FL	♂	0.667–0.717 (0.695) (±0.026) [3] {0.669–0.720} (0.037)	0.711–0.795 (0.754) (±0.060) [2] {0.693–0.813} (0.079)	0.837–0.850 (0.843) (±0.007) [3] {0.836–0.849} (0.008)
	♀	0.648–0.690 (0.668) (±0.021) [3] {0.647–0.689} (0.031)	0.633–0.667 (0.650) (±0.024) [2] {0.626–0.674} (0.036)	0.739–0.762 (0.746) (±0.011) [4] {0.735–0.757} (0.015)
W/FL	♂	0.745–0.868 (0.824) (±0.069) [3] {0.755–0.893} (0.083)	0.756–0.841 (0.798) (±0.060) [2] {0.738–0.859} (0.076)	0.909–0.975 (0.946) (±0.034) [3] {0.912–0.979} (0.035)
	♀	0.759–0.784 (0.774) (±0.013) [3] {0.760–0.787} (0.017)	0.650–0.684 (0.667) (±0.024) [2] {0.643–0.691} (0.036)	0.870–0.913 (0.890) (±0.022) [4] {0.868–0.912} (0.025)
L/ML	♂	0.500–0.528 (0.512) (±0.014) [3] {0.497–0.526} (0.028)	0.516–0.547 (0.532) (±0.022) [2] {0.510–0.553} (0.041)	0.581–0.597 (0.591) (±0.009) [3] {0.582–0.601} (0.016)
	♀	0.473–0.500 (0.489) (±0.014) [3] {0.475–0.503} (0.020)	0.469–0.475 (0.472) (±0.004) [2] {0.468–0.476} (0.009)	0.515–0.540 (0.526) (±0.010) [4] {0.515–0.536} (0.020)
W/ML	♂	0.567–0.639 (0.607) (±0.036) [3] {0.570–0.643} (0.060)	0.548–0.578 (0.563) (±0.021) [2] {0.542–0.584} (0.037)	0.645–0.684 (0.664) (±0.020) [3] {0.644–0.683} (0.030)
	♀	0.550–0.580 (0.566) (±0.015) [3] {0.551–0.581} (0.026)	0.481–0.488 (0.484) (±0.004) [2] {0.480–0.489} (0.009)	0.603–0.646 (0.627) (±0.018) [4] {0.608–0.645} (0.029)
Segment III				
L/FL	♂	0.745–0.792 (0.766) (±0.024) [3] {0.742–0.790} (0.032)	0.822–0.864 (0.843) (±0.029) [2] {0.814–0.872} (0.035)	0.884–0.909 (0.898) (±0.013) [3] {0.885–0.910} (0.014)
	♀	0.704–0.725 (0.718) (±0.012) [3] {0.706–0.730} (0.017)	0.667–0.702 (0.684) (±0.025) [2] {0.659–0.709} (0.036)	0.804–0.826 (0.812) (±0.010) [4] {0.803–0.822} (0.012)
W/FL	♂	0.725–0.840 (0.790) (±0.063) [3] {0.735–0.862} (0.079)	0.756–0.818 (0.787) (±0.044) [2] {0.743–0.831} (0.056)	0.909–0.950 (0.930) (±0.020) [3] {0.909–0.950} (0.022)
	♀	0.724–0.784 (0.756) (±0.030) [3] {0.726–0.786} (0.040)	0.617–0.649 (0.633) (±0.023) [2] {0.610–0.656} (0.036)	0.851–0.891 (0.867) (±0.018) [4] {0.849–0.885} (0.020)
L/ML	♂	0.543–0.583 (0.564) (±0.020) [3] {0.544–0.585} (0.036)	0.594–0.597 (0.595) (±0.002) [2] {0.593–0.597} (0.004)	0.613–0.645 (0.630) (±0.016) [3] {0.614–0.646} (0.026)
	♀	0.514–0.536 (0.525) (±0.011) [3] {0.514–0.536} (0.022)	0.494–0.500 (0.497) (±0.004) [2] {0.493–0.501} (0.009)	0.557–0.603 (0.572) (±0.021) [4] {0.551–0.593} (0.037)
W/ML	♂	0.552–0.611 (0.588) (±0.031) [3] {0.557–0.619} (0.053)	0.548–0.563 (0.555) (±0.010) [2] {0.545–0.565} (0.018)	0.645–0.667 (0.652) (±0.012) [3] {0.640–0.665} (0.019)
	♀	0.525–0.580 (0.553) (±0.027) [3] {0.526–0.580} (0.050)	0.457–0.463 (0.460) (±0.004) [2] {0.456–0.464} (0.009)	0.588–0.635 (0.611) (±0.025) [4] {0.586–0.636} (0.041)
Segment IV				
L/FL	♂	0.922–1.000 (0.967) (±0.041) [3] {0.926–1.008} (0.042)	1.000–1.091 (1.045) (±0.064) [2] {0.981–1.110} (0.061)	1.116–1.136 (1.126) (±0.010) [3] {1.116–1.136} (0.009)
	♀	0.852–0.931 (0.895) (±0.040) [3] {0.855–0.935} (0.045)	0.833–0.877 (0.855) (±0.031) [2] {0.824–0.886} (0.036)	1.000–1.048 (1.028) (±0.022) [4] {1.006–1.050} (0.021)
W/FL	♂	0.706–0.792 (0.753) (±0.044) [3] {0.709–0.797} (0.058)	0.711–0.772 (0.742) (±0.044) [2] {0.698–0.785} (0.059)	0.861–0.925 (0.883) (±0.036) [3] {0.847–0.919} (0.041)
	♀	0.724–0.745 (0.737) (±0.011) [3] {0.726–0.748} (0.015)	0.600–0.632 (0.616) (±0.022) [2] {0.593–0.638} (0.036)	0.830–0.857 (0.846) (±0.011) [4] {0.834–0.857} (0.014)
L/ML	♂	0.700–0.736 (0.713) (±0.020) [3] {0.692–0.733} (0.029)	0.726–0.750 (0.738) (±0.017) [2] {0.721–0.755} (0.023)	0.774–0.806 (0.790) (±0.016) [3] {0.774–0.806} (0.020)
	♀	0.622–0.675 (0.654) (±0.029) [3] {0.626–0.683} (0.044)	0.617–0.625 (0.621) (±0.005) [2] {0.616–0.627} (0.009)	0.706–0.762 (0.724) (±0.026) [4] {0.698–0.750} (0.036)
W/ML	♂	0.537–0.583 (0.555) (±0.025) [3] {0.529–0.580} (0.045)	0.516–0.531 (0.524) (±0.011) [2] {0.513–0.534} (0.020)	0.597–0.649 (0.620) (±0.027) [3] {0.593–0.646} (0.043)
	♀	0.525–0.551 (0.539) (±0.013) [3] {0.526–0.552} (0.024)	0.444–0.450 (0.447) (±0.004) [2] {0.444–0.451} (0.009)	0.574–0.619 (0.596) (±0.019) [4] {0.577–0.615} (0.032)
Segment V				
L/FL	♂	1.569–1.660 (1.610) (±0.047) [3] {1.563–1.656} (0.029)	1.600–1.750 (1.675) (±0.106) [2] {1.570–1.781} (0.063)	1.818–1.860 (1.843) (±0.022) [3] {1.821–1.865} (0.012)
	♀	1.529–1.574 (1.546) (±0.024) [3] {1.522–1.570} (0.016)	1.333–1.491 (1.412) (±0.112) [2] {1.301–1.524} (0.079)	1.660–1.739 (1.702) (±0.034) [4] {1.669–1.736} (0.020)
W/FL	♂	0.667–0.760 (0.727) (±0.052) [3] {0.675–0.780} (0.072)	0.667–0.727 (0.697) (±0.043) [2] {0.654–0.740} (0.061)	0.837–0.850 (0.843) (±0.007) [3] {0.836–0.849} (0.008)
	♀	0.690–0.706 (0.700) (±0.009) [3] {0.691–0.700} (0.013)	0.567–0.596 (0.582) (±0.021) [2] {0.560–0.603} (0.036)	0.787–0.826 (0.812) (±0.018) [4] {0.794–0.831} (0.023)
L/ML	♂	1.143–1.222 (1.186) (±0.040) [3] {1.146–1.227} (0.034)	1.161–1.203 (1.182) (±0.030) [2] {1.153–1.212} (0.025)	1.290–1.298 (1.293) (±0.005) [3] {1.288–1.298} (0.004)
	♀	1.113–1.149 (1.131) (±0.018) [3] {1.112–1.149} (0.016)	0.988–1.063 (1.025) (±0.053) [2] {0.972–1.078} (0.052)	1.147–1.270 (1.199) (±0.052) [4] {1.147–1.251} (0.043)
W/ML	♂	0.507–0.556 (0.535) (±0.025) [3] {0.510–0.560} (0.047)	0.484–0.500 (0.492) (±0.011) [2] {0.481–0.503} (0.023)	0.581–0.597 (0.591) (±0.009) [3] {0.582–0.601} (0.016)
	♀	0.500–0.522 (0.512) (±0.011) [3] {0.501–0.523} (0.021)	0.420–0.425 (0.422) (±0.004) [2] {0.410–0.426} (0.009)	0.544–0.603 (0.572) (±0.027) [4] {0.546–0.599} (0.046)

Metasomal Segment Widths Compared to Fixed Finger Length

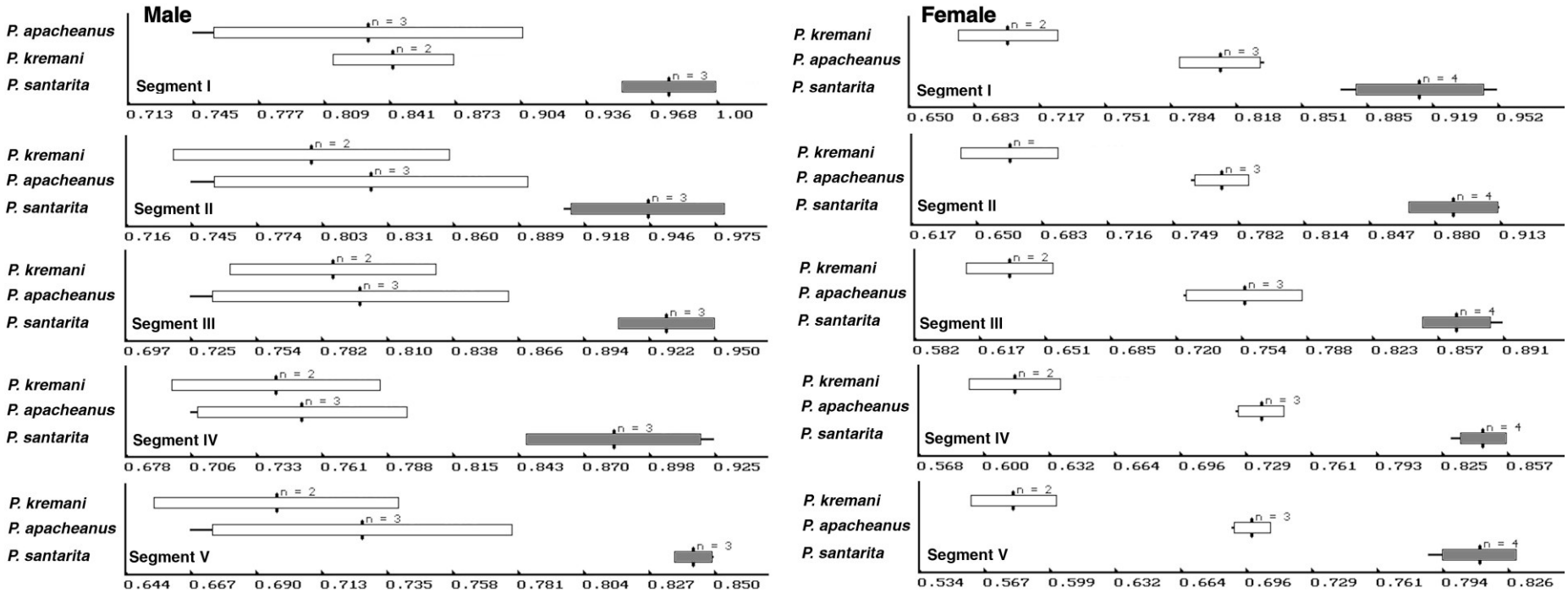

Figure B-2: Histograms demonstrate that *P. santarita* (dark bars) has the shortest chelal fixed fingers when the metasomal segment widths are compared to the fixed finger length.

MVD Comparisons of Chelal Finger Lengths Compared to Metasomal Segment Lengths and Widths

The following data demonstrates that *P. santarita* has the shortest chelal fingers, in particular, the fixed finger. Also, when the fixed finger is compared to the width of a metasomal segment, *P. santarita* exhibits, in most cases, the largest MVD (eighteen out of twenty). See above histogram.

Segment	**I**				**II**				**III**				**IV**				**V**			
***P. santarita* compared to *P. apacheanus*:**																				
	L/FL	**W/FL**	**L/ML**	**W/ML**	**L/FL**	**W/FL**	**L/ML**	**W/ML**	**L/FL**	**W/FL**	**L/ML**	**W/ML**	**L/FL**	**W/FL**	**L/ML**	**W/ML**	**L/FL**	**W/FL**	**L/ML**	**W/ML**
Male	0.133	0.176	0.078	0.121	0.213	0.147	0.155	0.094	0.172	0.164	0.116	0.110	0.164	0.173	0.109	0.117	0.145	0.159	0.090	0.105
Female	0.110	0.127	0.070	0.085	0.117	0.150	0.076	0.108	0.131	0.147	0.090	0.105	0.149	0.148	0.107	0.106	0.101	0.161	0.061	0.118
***P. santarita* compared to *P. kremani*:**																				
	L/FL	**W/FL**	**L/ML**	**W/ML**	**L/FL**	**W/FL**	**L/ML**	**W/ML**	**L/FL**	**W/FL**	**L/ML**	**W/ML**	**L/FL**	**W/FL**	**L/ML**	**W/ML**	**L/FL**	**W/FL**	**L/ML**	**W/ML**
Male	0.004	0.159	–0.004	0.152	0.119	0.185	0.113	0.178	0.065	0.182	0.058	0.174	0.077	0.190	0.071	0.183	0.100	0.209	0.094	0.202
Female	0.173	0.301	0.138	0.262	0.148	0.334	0.113	0.294	0.187	0.370	0.151	0.329	0.202	0.373	0.166	0.332	0.205	0.397	0.170	0.355

Fixed Finger *MD* Counts

Raw data broken down by sex, right and left chela, and *MD* denticle rows, one through six, *MD*–1 the most distal.

	MD–1	*MD*–2	*MD*–3	*MD*–4	*MD*–5	*MD*–6	Total
P. apacheanus							
Male							
right:	7	8	11	8	9	18	61
left:	6	9	11	8	9	17	60
right:	7	9	9	11	10	23	69
left:	7	9	10	12	12	22	72
right:	6	8	9	11	10	21	65
left:	5	8	9	12	9	21	64
	5–7 (6.333)	8–9 (8.500)	9–11 (9.833)	8–12 (10.333)	9–12 (9.833)	17–23 (18.667)	60–72 (65.167)
Female							
right:	6	9	9	10	11	23	68
left:	8	7	10	8	12	20	65
right:	6	8	9	11	11	16	61
left:	7	8	9	11	11	18	64
right:	6	10	8	10	9	21	64
left:	7	9	10	9	8	22	65
	6–8 (6.667)	7–10 (8.500)	8–10 (9.167)	8–11 (9.833)	8–12 (10.333)	16–23 (20.000)	61–68 (64.500)
P. kremani							
Male							
right:	6	7	9	7	8	15	52
left:	6	7	9	8	7	15	52
right:	6	7	7	8	9	14	51
left:	6	7	8	10	8	15	54
	6–6 (6.000)	7–7 (7.000)	7–9 (8.250)	7–10 (8.250)	7–9 (8.000)	14–15 (14.750)	51–54 (52.250)
Female							
right:	7	8	9	8	9	21	62
left:	7	7	8	10	9	19	60
right:	6	7	9	9	9	19	59
left:	6	7	9	10	10	19	61
right:	7	8	8	8	10	16	57
left:	8	8	9	8	10	16	59
	6–8 (6.833)	7–8 (7.500)	8–9 (8,667)	8–10 (8.833)	9–10 (9.500)	16–21 (18.333)	57–62 (59.667)

	MD–1	*MD*–2	*MD*–3	*MD*–4	*MD*–5	*MD*–6	Total
P. santarita							
Male							
right:	5	6	8	6	8	16	49
left:	6	6	8	8	8	13	49
right:	4	6	9	7	7	13	46
left:	5	6	7	8	8	14	48
right:	5	8	9	7	8	13	50
left:	4	7	9	7	8	15	50
	4–6 (4.833)	6–8 (6.500)	7–9 (8.333)	6–8 (7.167)	7–8 (7.833)	13–16 (14.000)	46–50 (48.667)
Female							
right:	5	6	7	7	8	15	48
left:	5	7	9	9	5	14	49
right:	4	6	8	8	7	14	47
left:	5	5	7	8	8	15	48
right:	5	6	9	8	8	14	50
left:	5	7	7	8	7	15	49
right:	6	7	8	7	9	15	52
left:	5	7	9	7	8	17	53
	4–6 (5.000)	5–7 (6.375)	7–9 (8.000)	7–9 (7.750)	5–9 (7.500)	14–17 (14.875)	47–53 (49.500)

	P. apacheanus	***P. kremani***	***P. santarita***
♂	60–72 (65.167) (±4.622) [6] {60.544–69.789} (0.071)	51–54 (52.250) (±1.258) [4] {50.992–53.508} (0.024)	46–50 (48.667) (±1.506) [6] {47.161–50.172} (0.031)
♀	61–68 (64.500) (±2.258) [6] {62.242–66.758} (0.035)	57–62 (59.667) (±1.751) [6] {57.916–61.418} (0.029)	47–53 (49.500) (±2.070) [8] {47.430–51.570} (0.042)
♂&♀	60–72 (64.833) (±3.486) [12] {61.347–68.319} (0.054)	51–62 (56.700) (±4.111) [10] {52.589–60.811} (0.073)	46–53 (49.143) (±1.834) [14] {35.143–50.977} (0.037)

Fixed Finger *MD* Counts MVD%

	P. apacheanus	***P. kremani***	***P. santarita***
P. apacheanus			
♂	–	0.24721	0.33904
♀	–	0.08101	0.30303
♂&♀	–	0.14345	0.20844
P. kremani			
♂	–	–	0.07363
♀	–	–	0.20539
♂&♀	–	–	0.15378

Metasomal Segments Length/Width MVD%

	I	II	III	IV	V	Average
	P. kremani* vs. *P. apacheanus					
♂:	0.107	0.117	0.114	0.096	0.083	0.103
♀:	0.093	0.128	0.137	0.143	0.098	0.120
	P. kremani* vs. *P. santarita					
♂:	0.155	0.058	0.110	0.104	0.099	0.105
♀:	0.109	0.162	0.154	0.142	0.158	0.145

Comparison of Chelal Fixed Finger Lengths Between Sexes

The length/width of the five metasomal segments are compared to the chelal fixed finger length demostrating that the female of *P. kremani* has a longer fixed finger.

P. kremani	*P. apacheanus*	*P. santarita*
I–L/FL: **MVD = 0.212**	I–L/FL: **MVD = 0.017**	I–L/FL: **MVD = 0.037**
male 0.67–0.68 (0.674) (±0.011) [2] {0.66–0.68} (0.016)	male 0.59–0.60 (0.597) (±0.008) [3] {0.59–0.61} (0.014)	male 0.65–0.72 (0.677) (±0.039) [3] {0.64–0.72} (0.057)
female 0.53–0.58 (0.556) (±0.032) [2] {0.52–0.59} (0.058)	female 0.55–0.62 (0.587) (±0.036) [3] {0.55–0.62} (0.061)	female 0.64–0.67 (0.652) (±0.012) [4] {0.64–0.66} (0.018)
I–W/FL: **MVD = 0.202**	I–W/FL: **MVD= 0.025**	I–W/FL: **MVD = 0.071**
male 0.82–0.86 (0.843) (±0.029) [2] {0.81–0.87} (0.035)	male 0.75–0.89 (0.831) (±0.075) [3] {0.76–0.91} (0.091)	male 0.95–1.00 (0.977) (±0.023) [3] {0.95–1.00} (0.023)
female 0.68–0.72 (0.701) (±0.025) [2] {0.68–0.73} (0.036)	female 0.79–0.83 (0.810) (±0.021) [3] {0.79–0.83} (0.026)	female 0.87–0.95 (0.913) (±0.033) [4] {0.88–0.95} (0.036)
II–L/FL: **MVD = 0.159**	II–L/FL: **MVD = 0.040**	II–L/FL: **MVD = 0.129**
male 0.71–0.80 (0.753) (±0.060) [2] {0.69–0.81} (0.079)	male 0.67–0.72 (0.695) (±0.026) [3] {0.67–0.72} (0.037)	male 0.84–0.85 (0.843) (±0.007) [3] {0.84–0.85} (0.008)
female 0.63–0.67 (0.650) (±0.024) [2] {0.63–0.67} (0.036)	female 0.65–0.69 (0.668) (±0.021) [3] {0.65–0.69} (0.031)	female 0.74–0.76 (0.746) (±0.011) [4] {0.74–0.76} (0.014)
II–W/FL: **MVD = 0.197**	II–W/FL: **MVD = 0.066**	II–W/FL: **MVD = 0.063**
male 0.76–0.84 (0.798) (±0.060) [2] {0.74–0.86} (0.076)	male 0.75–0.87 (0.824) (±0.069) [3] {0.76–0.89} (0.083)	male 0.91–0.98 (0.946) (±0.034) [3] {0.91–0.98} (0.036)
female 0.65–0.68 (0.667) (±0.024) [2] {0.64–0.69} (0.036)	female 0.76–0.78 (0.774) (±0.013) [3] {0.76–0.79} (0.017)	female 0.87–0.91 (0.890) (±0.022) [4] {0.87–0.91} (0.025)
III–L/FL: **MVD = 0.232**	III–L/FL: **MVD = 0.067**	III–L/FL: **MVD = 0.105**
male 0.82–0.86 (0.843) (±0.029) [2] {0.81–0.87} (0.035)	male 0.75–0.79 (0.766) (±0.024) [3] {0.74–0.79} (0.032)	male 0.88–0.91 (0.898) (±0.013) [3] {0.88–0.91} (0.014)
female 0.67–0.70 (0.684) (±0.025) [2] {0.66–0.71} (0.036)	female 0.70–0.73 (0.718) (±0.012) [3] {0.71–0.73} (0.017)	female 0.80–0.83 (0.812) (±0.010) [4] {0.80–0.82} (0.012)
III–W/FL: **MVD = 0.243**	III–W/FL: **MVD = 0.056**	III–W/FL: **MVD = 0.072**
Male 0.76–0.82 (0.787) (±0.044) [2] {0.74–0.83} (0.056)	male 0.73–0.84 (0.799) (±0.063) [3] {0.74–0.86} (0.079)	male 0.91–0.95 (0.930) (±0.020) [3] {0.91–0.95} (0.022)
female 0.62–0.65 (0.633) (±0.023) [2] {0.61–0.66} (0.036)	female 0.72–0.78 (0.756) (±0.030) [3] {0.73–0.79} (0.040)	female 0.85–0.89 (0.867) (±0.018) [4] {0.85–0.89} (0.020)
IV–L/FL: **MVD = 0.222**	IV–L/FL: **MVD = 0.081**	IV–L/FL: **MVD = 0.095**
male 1.00–1.09 (1.045) (±0.064) [2] {0.98–1.11} (0.061)	male 0.92–1.00 (0.967) (±0.041) [3] {0.93–1.01} (0.042)	male 1.12–1.14 (1.126) (±0.010) [3] {1.12–1.14} (0.009)
female 0.83–0.88 (0.855) (±0.031) [2] {0.82–0.89} (0.036)	female 0.85–0.93 (0.895) (±0.040) [3] {0.85–0.94} (0.045)	female 1.00–1.05 (1.028) (±0.022) [4] {1.01–1.05} (0.021)
IV–W/FL: **MVD = 0.205**	IV–W/FL: **MVD = 0.022**	IV–W/FL: **MVD = 0.044**
male 0.71–0.77 (0.742) (±0.044) [2] {0.70–0.79} (0.059)	male 0.71–0.79 (0.753) (±0.044) [3] {0.71–0.80} (0.058)	male 0.86–0.93 (0.883) (±0.036) [3] {0.85–0.92} (0.041)
female 0.60–0.63 (0.616) (±0.022) [2] {0.59–0.64} (0.036)	female 0.72–0.75 (0.737) (±0.011) [3] {0.73–0.75} (0.015)	female 0.83–0.86 (0.846) (±0.011) [4] {0.83–0.86} (0.014)
V–L/FL: **MVD = 0.186**	V–L/FL: **MVD = 0.041**	V–L/FL: **MVD = 0.083**
Male 1.60–1.75 (1.675) (±0.106) [2] {1.57–1.78} (0.063)	male 1.57–1.66 (1.610) (±0.047) [3] {1.56–1.66} (0.029)	male 1.82–1.86 (1.843) (±0.022) [3] {1.82–1.86} (0.012)
Female 1.33–1.49 (1.412) (±0.112) [2] {1.30–1.52} (0.079)	female 1.53–1.57 (1.546) (±0.024) [3] {1.52–1.57} (0.016)	female 1.66–1.74 (1.702) (±0.034) [4] {1.67–1.74} (0.020)
V–W/FL: **MVD = 0.198**	V–W/FL: **MVD = 0.039**	V–W/FL: **MVD = 0.038**
male 0.67–0.73 (0.697) (±0.043) [2] {0.65–0.74} (0.061)	male 0.67–0.76 (0.727) (±0.052) [3] {0.67–0.78} (0.072)	male 0.84–0.85 (0.843) (+–0.007) [3] {0.84–0.85} (0.008)
female 0.57–0.60 (0.582) (±0.021) [2] {0.56–0.60} (0.036)	female 0.69–0.71 (0.700) (±0.009) [3] {0.69–0.71} (0.013)	female 0.79–0.83 (0.812) (+–0.018) [4] {0.79–0.83} (0.023)
MVDs 15.9 – 24.3 (20.56) %	**1.7 – 8.1 (4.54) %**	**3.7 – 12.9 (7.37) %**

Pectinal Tooth Count Ranges

	Male	Female
***P. apacheanus*:**	10–12 (10.600) (±0.699) [10]	9–11 (9.722) (±0.575) [18]
***P. santarita*:**	10–12 (11.000) (±0.555) [14]	8–10 (9.000) (±0.378) [29]
***P. kremani*:**	11–12 (11.214) (±0.426) [14]	9–10 (9.469) (±0.507) [32]

The pectinal tooth counts presented above are based on the eighteen specimens analysed above as well as additional material including the holotype female and paratype male reported by Gertsch & Soleglad (1972: tab. 2).